2021
Proceedings of the
13th Joint Seminar

×

Kunsan National University *Yamaguchi University*

16th September, 2021

Online

Foreword

On behalf of our faculty members, I would like to extent my most sincere welcome to the members from Kunsan National University. Due to COVID-19 situation this seminar will be held online. While recognizing the new possibilities of online seminars, I also feel the importance of face-to-face meeting and talking as before COVID-19 situation.

As the ancient Romans once said, “Rome was not built in a day”.

We have step by step developed a good relationship between Kunsan National University and Yamaguchi University. Since the academic exchange agreement was established between Kunsan National University and Yamaguchi University in 2010, mutual student and academic exchange both universities has been conducted since 2006. As the Dean of Faculty of Engineering of Yamaguchi University, this is a great honor and pleasure for me to meet you all participants today and attend the opening of this online joint seminar in the attendance from Kunsan National University.

This joint seminar covers excellent and meaningful research topics between us. I believe that this seminar becomes a precious opportunity to comprehend existing problems and try to determine new directions and visions for diverse research field in engineering. Also I wish this seminar becomes informative, productive and entertaining both scientifically and culturally provision for new friendship between Kunsan National University and Yamaguchi University. I also hope that this exchange program will be handed over to the next generation researchers and students of both universities.

Finally, I would like to also express my sincere thankfulness to the contributors of this joint seminar who made all this possible and I wish you all have fruitful time with this online seminar.

Thank you very much.

Hiromori Tsutsumi Ph.D.
Dean
Faculty of Engineering, Yamaguchi University

Contents

Foreword i

Contents ii

Joint Seminar 1

Abstracts of Invited Presentation 3

1. Review of Engineering Education under COVID-19 4
   Prof. Yong-yee Kim (Dept. of Architecture and Building Eng., KSNU) and
   Prof. Junghoon Joo (Dept. of Materials Science and Eng., KSNU)

2. Online Science Learning in Yamaguchi University 6
   Prof. Takayuki Narumi (Dept. of Applied Science, YU)

3. Characterization on Cell Performance for Electrode and Operation Parameters in Anion Exchange Membrane-unitized Regenerative Fuel Cells 8
   Prof. Joongpyo Shim (Dept. of Chemical Eng., KSNU)

4. Effect of Electrolysis Cell Structure and Flow Conditions on the Seawater Electrolysis 10
   Prof. Nobutaka Endo (Dept. of Sustainable Environmental Eng., YU)

5. Leaf Spot Attention Networks for Leaf Diseases Identification and Detection 12
   Prof. Chang-Hwan Son (Dept. of Software Convergence Eng., KSNU)

6. A Study on Medical Computer-Aided Diagnosis for a Small Number of Labeled Training Data 14
   Prof. Shingo Mabu (Dept. of Information Science and Eng., YU)

7. Low-Cost Simple Look-up Table based PMSM Drive Considering DC-link Voltage Variation 16
   Prof. Junghyo Lee (Dept. of Electrical Eng., KSNU)

8. On Dual System Representation and Prediction Method for Data-Driven Estimation 19
   Prof. Ryosuke Adachi (Dept. of Electrical and Electronic Eng., YU)

Student Poster Presentations 21

1. Grafted Polymer Chain-introduced Monolithic Silica Columns for Separation of Vaccine Virus 22
   Junghu Lee (Dept. of Applied Chemistry, YU)

2. A Numerical Study on the Wave Characteristics Generated by Double Flap Type 23
   Yan Kaicheng (Dept. of Naval Architecture, KSNU)

3. Effect of Martensite Low Alloy Steel on Hydrogen Sensitivity 24
   Takuma Ishibashi (Division of Mechanical Eng., YU)

4. Numerical Study of the Free Decay Test for the Semi-Submersible Structures of Floating Offshore Wind Turbines 25
   Se-Bum Oh (Dept. of Naval Architecture, KSNU)

5. Iron and Manganese Surface Treatment on Anode Electrodes in Plant Microbial Fuel Cells for Improved Bio-Electricity Generation 26
   Shohei Uramoto (Division of Construction and Environmental Eng., YU)

6. Structural Design and Analysis of Gear Pump for Mechanical System 27
   Yonggyu Lee (Dept. of Mechanical Eng., KSNU)

7. Method for Animating Water-Flow in an Illustration 28
   Yusuke Kawazu (Division of Electrical, Electronic and Information Eng., YU)

8. Performance Analysis of Consequent Pole Vernier Machine for MW Scale Wind Power Generator 29
   Abdur Rehman (Dept. of Electrical Eng., KSNU)

9. Combination of High-Temperature Fermentation and Membrane Separation for Bioethanol Production 30
   Yu Shimada (Division of Applied Chemistry, YU)

10. Battery Cell Balancing Unit for Manufacturing Industry 31
    Hyeon-Sik Kang (Dept. of Electrical Eng., KSNU)

11. Fall Detection based on AutoEncoder with Obrid-Sensor 32
    Taiki Sunakawa (Division of Electrical, Electronic and Information Eng., YU)

12. Numerical Simulation of the Hazardous Gas Leakage Accident in Saemangum Industrial Park 33
    Jaebeen Lee (Dept. of Material Science and Eng., KSNU)

13. Disaster Prevention Awareness Questionnaire Survey for Residents of Storm Surge Hazard Area - A Case Study of Ube City, Yamaguchi Prefecture - 34
    Ayame Tamuro (Division of Construction and Environmental Eng., YU)

14. A Graph Theory-based User Association Scheme for Device-to-Device Task Offloading in 5G Networks 35
    Ralph Voltaire Dayot (School of Computer, Information & Communication Eng., KSNU)

13th JOINT SEMINAR

16th September, 2021

(Online)

9:00-9:15 **Opening Ceremony**

Welcome address Prof. Masaaki Oka, President of Yamaguchi University (YU)

Congratulatory address Prof. Byong-Sun Kuack, President of Kunsan National University (KSNU)

Invited Presentations I Chair: Prof. Izumi Kumakiri (Dept. of Sustainable Environmental Eng., YU)

Educational topic

9:15-9:35 **Review of Engineering Education under COVID-19**
Prof. Yong-yee Kim (Dept. of Architecture and Building Eng., KSNU) and
Prof. Junghoon Joo (Dept. of Materials Science and Eng., KSNU)

9:35-9:55 **Online Science Learning in Yamaguchi University**
Prof. Takayuki Narumi (Dept. of Applied Science, YU)

Research topic

9:55-10:15 **Characterization on Cell Performance for Electrode and Operation Parameters in Anion Exchange Membrane-unitized Regenerative Fuel Cells**
Prof. Joongpyo Shim (Dept. of Chemical Eng., KSNU)

10:15-10:35 **Effect of Electrolysis Cell Structure and Flow Conditions on the Seawater Electrolysis**
Prof. Nobutaka Endo (Dept. of Sustainable Environmental Eng., YU)

10:35-11:00 Break

Invited Presentations II Chair: Prof. Se-Myong Chang (Dept. of Mechanical Eng. / Dean of Convergence Eng., KSNU)

Research topic

11:00-11:20 **Leaf Spot Attention Networks for Leaf Diseases Identification and Detection**
Prof. Chang-Hwan Son (Dept. of Software Convergence Eng., KSNU)

11:20-11:40 **A Study on Medical Computer-Aided Diagnosis for a Small Number of Labeled Training Data**
Prof. Shingo Mabu (Dept. of Information Science and Eng., YU)

11:40-12:00 **Low-Cost Simple Look-up Table based PMSM Drive Considering DC-link Voltage Variation**
Prof. Junghyo Lee (Dept. of Electrical Eng., KSNU)

12:00-12:20 **On Dual System Representation and Prediction Method for Data-Driven Estimation**
Prof. Ryosuke Adachi (Dept. of Electrical and Electronic Eng., YU)

12:20-13:30 Lunch on your own

Student Poster Presentations I Chair: Prof. Ryuichi Komatsu (Dept. of Applied Chemistry, YU)

13:30-13:40 **Grafted Polymer Chain-introduced Monolithic Silica Columns for Separation of Vaccine Virus**
Junghu Lee (Dept. of Applied Chemistry, YU)

13:40-13:50 **A Numerical Study on the Wave Characteristics Generated by Double Flap Type**
Yan Kaicheng (Dept. of Naval Architecture, KSNU)

13:50-14:00 **Effect of Martensite Low Alloy Steel on Hydrogen Sensitivity**
Takuma Ishibashi (Division of Mechanical Eng., YU)

14:00-14:10 **Numerical Study of the Free Decay Test for the Semi-Submersible Structures of Floating Offshore Wind Turbines**
Se-Bum Oh (Dept. of Naval Architecture, KSNU)

14:10-14:20 **Iron and Manganese Surface Treatment on Anode Electrodes in Plant Microbial Fuel Cells for Improved Bio-Electricity Generation**
Shohei Uramoto (Division of Construction and Environmental Eng., YU)

14:20-14:30 **Structural Design and Analysis of Gear Pump for Mechanical System**
Yonggyu Lee (Dept. of Mechanical Eng., KSNU)

14:30-14:40 **Method for Animating Water-Flow in an Illustration**
Yusuke Kawazu (Division of Electrical, Electronic and Information Eng., YU)

14:40-15:00 Break

Student Poster Presentations II Chair: Prof. Minchul Ahn (Dept. of Electrical Eng., KSNU)

15:00-15:10 **Performance Analysis of Consequent Pole Vernier Machine for MW Scale Wind Power Generator**
Abdur Rehman (Dept. of Electrical Eng., KSNU)

15:10-15:20 **Combination of High-Temperature Fermentation and Membrane Separation for Bioethanol Production**
Yu Shimada (Division of Applied Chemistry, YU)

15:20-15:30 **Battery Cell Balancing Unit for Manufacturing Industry**
Hyeon-Sik Kang (Dept. of Electrical Eng., KSNU)

15:30-15:40 **Fall Detection based on AutoEncoder with Obrid-Sensor**
Taiki Sunakawa (Division of Electrical, Electronic and Information Eng., YU)

15:40-15:50 **Numerical Simulation of the Hazardous Gas Leakage Accident in Saemangum Industrial Park**
Jaebeen Lee (Dept. of Material Science and Eng., KSNU)

15:50-16:00 **Disaster Prevention Awareness Questionnaire Survey for Residents of Storm Surge Hazard Area - A Case Study of Ube City, Yamaguchi Prefecture -**
Ayame Tamuro (Division of Construction and Environmental Eng., YU)

16:00-16:10 **A Graph Theory-based User Association Scheme for Device-to-Device Task Offloading in 5G Networks**
Ralph Voltaire Dayot (School of Computer, Information & Communication Eng., KSNU)

16:10-16:30 Break

16:30-17:00 **Closing Ceremony**

Award Announcement

Closing remarks Prof. Junghoon Joo, Dean of College of Eng., KSNU
Prof. Hiromori Tsutsumi, Dean of Faculty of Eng., YU

Abstracts of Invited Presentation

Review of Engineering Education under COVID-19

KIM Yong-Yee[1] and JOO Junghoon[2]

[1]Dept. of Architecture and Building Eng., KSNU
[2]Dept. of Materials Science and Eng., KSNU
Daehak-ro 558, Gunsan-si, Jeollabuk-do, 54150 Republic of Korea
[1]E-mail: yongyee.kim@kunsan.ac.kr, [2]E-mail: jhjoo@kunsan.ac.kr

This paper covers review and several questions of engineering education under COVID-19 during one and half year.1) Were university students self-directed learner or trained passive learner? Some said that it was so hard to learn with less autonomy. In general, time spent for study were not increased as expected. But collaborative learning and interaction with diverse others were greatly decreased (Fig. 1).

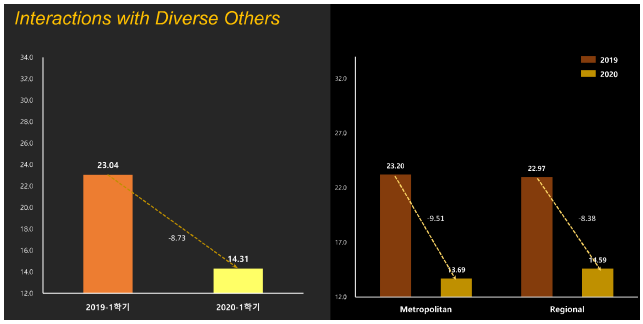

Fig. 1 Interactions with diverse others

2)Were KSNU students different from other university students? No, furthermore almost survey items are inferior to others, as shown in Fig. 2, especially during first semester in 2020, in which world-wide online education started because of COVID-19.

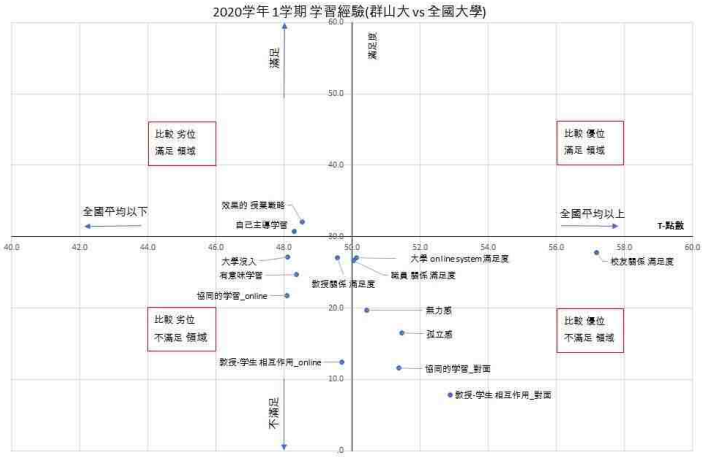

Fig. 2 Student Engagement Comparison between KSNU and other universities

After first semester in 2020, student satisfaction with online LMS(learning management system) was increased more than other universities, as shown in Fig. 3.

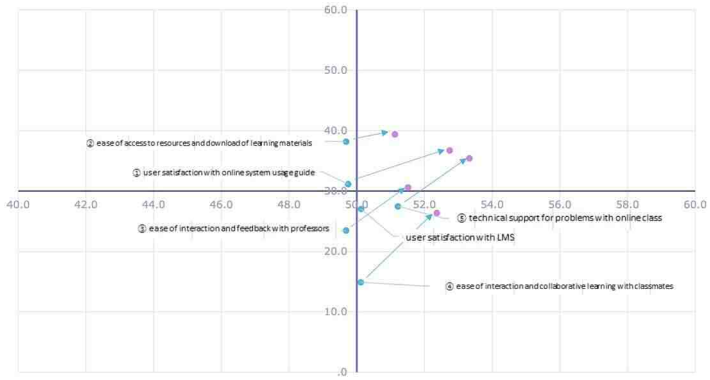

Fig. 3. User satisfaction with LMS

3)How was student engagement in KSNU? What were better than others? What are lessons and implications of online learning engagement under COVID-19? According to KNSSE, collaborative learning, interaction with diverse others, interaction with professors, quality of interaction with peers, professors and staffs, and supportive environments are comparatively superior to others. But self-efficacy for academic attainment, vocational maturity, and etc. are comparatively inferior.

References

1. S. Bae, “Presents and Assignments that COVID-19 gave universities,” Korea Educational Research Association,Special Session, 2020. 6.
2. Education and Future Research Institue, “2020 KNSSE Report-KSNU,” Korea National Survey of Student Engagement, 2020.6.
3. Education and Future Research Institue, “2020 KNSSE Report for Online Learning Engagement -KSNU,” Korea National Survey of Student Engagement, 2021.1

Online Science Learning in Yamaguchi University

Takayuki Narumi

Department of Applied Science, Yamaguchi University
Tokiwadai, 2-16-1, Ube 755-8611, Japan
E-mail: tnarumi@yamaguchi-u.ac.jp

Digest

This paper summarizes the online science learning in Yamaguchi University (YU), mainly focusing on the case of the Faculty of Engineering.

On April 7, 2020, a state of emergency was declared in some urban areas in Japan. On April 16, 2020, the declared area was expanded to include Yamaguchi Prefecture and the rest of Japan. YU has implemented fully online classes for the first semester of the 2020 academic year. Until the 2019 academic year, online education was offered only in a few subjects, and most students and faculty members had no experience with online courses. The problems in implementing online classes were the teaching skills of the faculty members and equipment such as servers. In response to these problems, a class-support task force was formed, headed by the Vice President of YU. The member actively shared information across faculties and departments on various issues (e.g., copyright issues for online materials, excessive reports, lack of relationship-building among students, etc.). Since the Center for Information Infrastructure (CII) staff also participated, we were able to have in-depth discussions on the performance requirements of the servers.

According to the Ministry of Education, Culture, Sports, Science and Technology (MEXT), there are two examples of online classes: (1) interactive classes using video conferencing tools such as Zoom, and (2) remote classes using on-demand video distribution. Based on these circumstances, the Faculty of Engineering held several study sessions on each class format to share the know-how of online classes among faculty members. The author was also a presenter at the study sessions and introduced various methods of creating on-demand videos for faculty members to choose from.

As for the server and other facilities, the CII was responsible for improving the

delivery performance of the existing Moodle, building a new video delivery server, and expanding the storage capacity. On the other hand, to reduce the number of simultaneous connections to the server, we also took measures such as staggering the connections to the server when multiple classes were overlapping. As a result of these efforts, the servers provided a stable online learning environment except for short-time failures.

The nationwide spread of online education has brought about irreversible changes in university education, and it will be necessary to update university education in response to these changes. The greatest advantage of online classes is the ability to learn without being restricted by time and place. This indicates the possibility of providing university education to, for example, working people who want to study at a university again. Such a movement is expected to spread nationwide, and it is necessary to explore the university's own initiatives in this context.

In the presentation, we would like to discuss the merits and demerits of online education and the prospects of online education by sharing case studies, mainly from YU.

Characterization on Cell Performance for Electrode and Operation Parameters in Anion Exchange Membrane-unitized Regenerative Fuel Cells

Joongpyo Shim[1] and Md. Masud Rana[1]

[1]Department of Chemical Engineering, Kunsan National University
Gunsan, Jeonbuk, 54150, Korea
[1]E-mail: jpshim@kunsan.ac.kr

Digest

In recent years, energy storage and conversion by electrochemical cells such as rechargeable and flow batteries, fuel cells and supercapacitors have been hot issues for saving energy. A regenerative fuel cell (RFC), one of fuel cell type, is a promising energy conversion system from hydrogen and oxygen to electricity, and vice versa. The RFC system has two unit of a water electrolyzer and a fuel cell. FC is unit for producing electricity using hydrogen and oxygen, and reversely, WE is unit for producing hydrogen and oxygen using electricity. This RFC system has distinctive advantages over rechargeable batteries with its long-term energy storage and high specific energy [1]. However, applications of the RFC system have been limited because of the high cost and complexity of the system. To resolve the problems, unitized regenerative fuel cells (URFC) has been developed in an integrated single unit that integrates a fuel cell and a water electrolyzer.

Proton exchange membrane based URFC (PEM-URFC) has been studied from early 1990s [2]. Nafion and platinum group metals (PGM) have been used as PEM and catalysts because of high ionic conductivity and catalytic activity, respectively. However, PEM-URFC has still had the limitation because of high cost of materials.

Anion exchange membrane (AEM) is OH^- ion (hydroxyl ion) conducting polymer which is one of key components in AEMFC or AEMWE, and should have high ionic conductivity, ultimately low gas permeability, non-electric conductivity, and mechanical/chemical stabilities. Recently, commercially available AEM, such as Tokuyama and Fumatech, was applied to AEMFC.

In this work, AEM-URFC will be fabricated with Fumapem as AEM, which was commercial product of Fumatech, and Pt/C as catalyst. The cell performance for FC

and WE mode will be characterized on electrode and operation parameters such as ionomer contents, catalyst loading, cell temperature, etc.

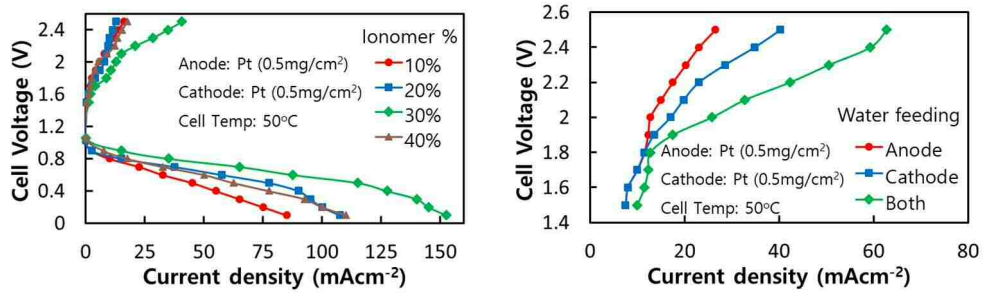

Fig. 1. Cell performance of AEM-URFC on ionomer content and water feeding.

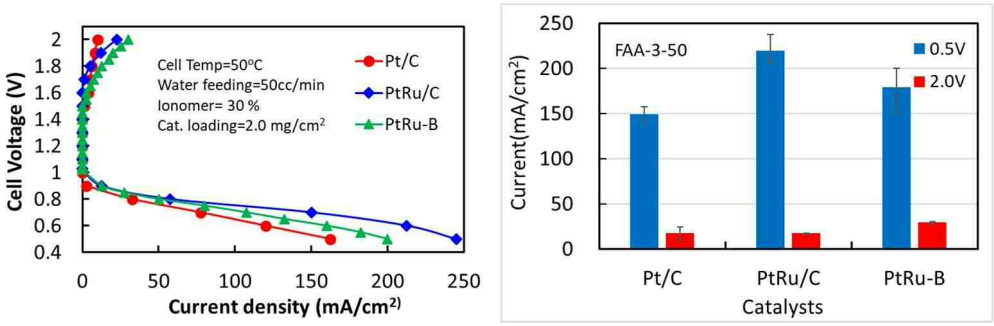

Fig. 2. Cell performance of AEM-URFC on different catalysts for bifunctional oxygen electrode.

References

1. S.-D. Yim, W.-Y. Lee, Y.-G. Yoon, Y.-J. Sohn, G.-G. Park, T.-H. Yang, C.-S. Kim, “Optimization of bifunctional electrocatalyst for PEM unitized regenerative fuel cell”, Electrochim. Acta, 50, 2004, 713-718
2. H.P. Dhar, “A unitized approach to regenerative solid polymer electrolyte fuel cells”, J. Appl. Electrochem. 23 (1993) 32.

Effect of Electrolysis Cell Structure and Flow Conditions on the Seawater Electrolysis

Nobutaka Endo* and Yuudai Okamoto

Department of Sustainable Environmental Engineering,
Yamaguchi University
Tokiwadai, 2-16-1, Ube 755-8611, Japan
*E-mail: n-endo@yamaguchi-u.ac.jp

Digest

Water electrolysis seems to be well established technology with high energy conversion efficiency. The biggest problem is high costs of electrical energy, especially in Japan. The seawater electrolysis is one of the solutions for reduction of costs because seawater is infinite natural source. In seawater electrolysis for energy production, a huge amount of chlorine emission is not allowed. But, appropriate amount of chlorine production can be used to sterilization and industrial source. In this study, we examined to the clarify the relation between the hydrogen, oxygen and chlorine evolution behavior and electrolyte and supply conditions (pH, concentration, flow rate, etc.). The flow-type electrolysis cell (Fig.1) was consisted that active area is 70cm^2 and flow path thickness is 5 mm.

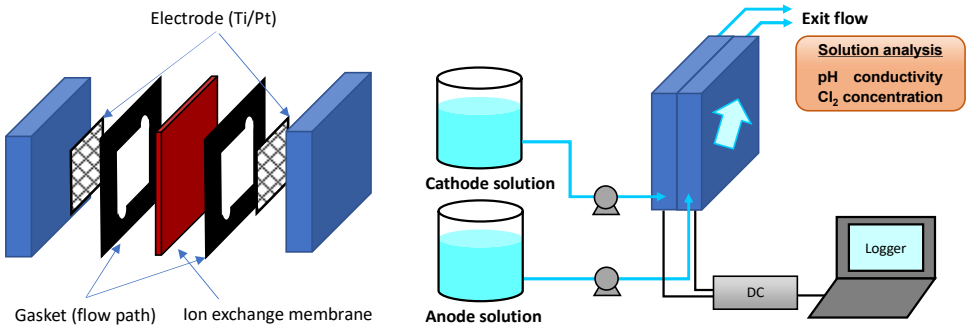

Fig. 1 Image diagram of flow cell (left) and experimental apparatus (right).

The experimentally observed the oxidation-reduction potentials (ORPs) of oxygen and chlorine evolution reaction are similar potentials in 3.5wt% NaCl solution (pH 6.5). Supposing that oxygen and chlorine evolution is competed against each other, chlorine evolution has priority due to the higher concentration of Cl- on the theoretical calculation. However, on this experiment (impressed current density; 7.14 mA/cm2, linear velocity; 1.78 cm/s), chlorine evolution is smaller than the calculated values (Fig.2). This tendency becomes remarkable with decreasing of flow rate and increasing of current density. It is considered that the water stream in such thin plate channel is preferentially flowed to flow direction. Hence, a portion of solution is flowed through on the electrode surface to outlet, and the solute concentration is changed notably by the electrolytic reaction. This distinction of concentrations is expanding by the difference of ionic mobility (Fig.3).

The electrolytic selectivity can be controlled by the cell structure and operating condition. This issue may be able to use the selectively-electrolytic electrode, it leads to achievement of the high oxygen-selectively sea water electrolysis.

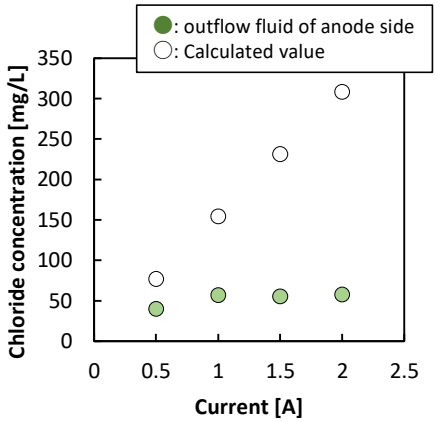

Fig.2 Relationship between chlorine concentrations in outflow fluid of anode and supplied current. (3.5 wt% NaCl, 50cc/min)

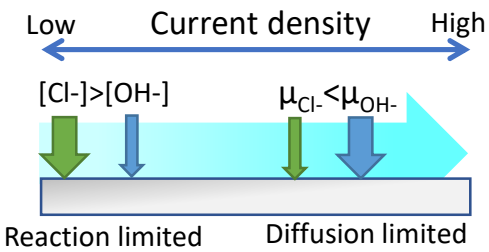

Fig. 3 Image of ionic mobility near the electrode surface.

Leaf Spot Attention Networks for Leaf Diseases Identification and Detection

Chang-Hwan Son

Department of Software Convergence Engineering, Kunsan National University
Daehak-ro 558, Gunsan-si 54150, Korea
E-mail: cson@kunsan.ac.kr

Digest

This study proposes a new attention-enhanced YOLO (AE-YOLO) model that incorporates a leaf spot attention mechanism based on regions-of-interest (ROI) feature extraction into the YOLO framework for leaf disease detection. Inspired by a previous study [1], which revealed that leaf spot attention based on the ROI-aware feature extraction can improve the leaf disease recognition accuracy significantly and outperform state-of-the-art deep learning models. This study extends the leaf spot attention model to leaf disease detection. The primary idea is that spot areas indicating leaf diseases appear only in leaves, whereas the background area does not contain useful information regarding leaf diseases. To increase the discriminative power of the feature extractor that is required in the object detection framework, it is essential to extract informative and discriminative features from the spot and leaf areas.

To realize this, a new ROI-aware feature extractor, that is, a spot feature extractor is designed. To divide the leaf image into spot, leaf, and background areas, the leaf segmentation module is first pretrained, and then spot feature encoding is applied to encode spot information. Next, the ROI-aware feature extractor is connected to an ROI-aware feature fusion layer to model the leaf spot attention mechanism, and to be joined with the YOLO detection subnetwork [2]. It is well known that the existing YOLO model [2] consists of a feature extractor and detection subnetwork. However, this YOLO model excludes leaf spot attention mechanisms, thus, it lacks the ability to find spot areas that are spatially important, and extract informative spot features. To complement this, the leaf spot attention mechanism needs to be incorporated into the YOLO network. As illustrated in Fig. 1, the proposed AE-YOLO model contains ROI-aware FES and ROI-aware feature fusion.

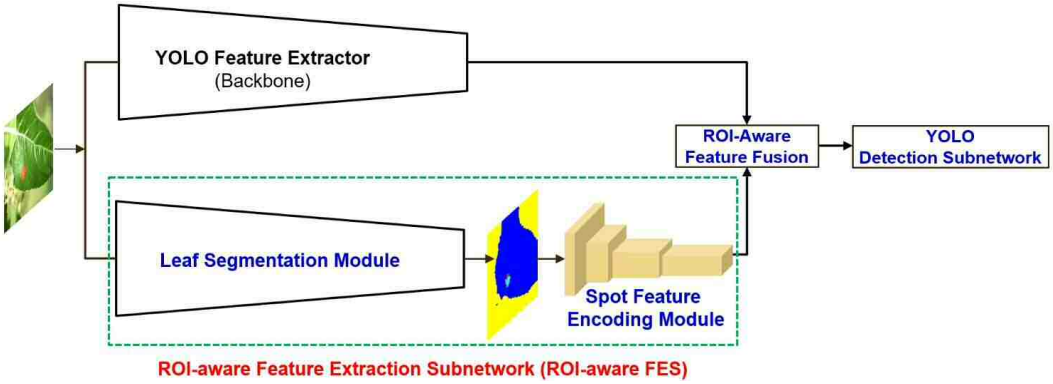

Fig. 1. Proposed attention-enhanced YOLO network for leaf diseases detection.

Fig. 2 illustrates the predicted bounding boxes with the proposed AE-YOLO. As illustrated in the figure, the proposed AE-YOLO can detect diseased leaves properly. In addition, the proposed AE-YOLO increases the average precision (AP) value by 6.1%, compared to the conventional YOLO. The AP value of the proposed method is 51.70. This result confirms that the ROI-aware FES and feature fusions have a significant effect on improving object detection performance. Therefore, the proposed spot feature extractor can improve leaf disease detection by boosting the discriminative power of spot features. In addition, the proposed attention-enhanced YOLO model outperforms the conventional YOLO model [2].

Fig. 2. Detection results; ground truth bounding boxes (upper row), predicted bounding boxes with the proposed AE-YOLO model (bottom row).

References

1. H.-J. Yu and C.-H. Son, “Leaf spot attention network for apple leaf disease identification,” In Proceedings of the IEEE Conference on Computer Vision and Pattern Recognition Workshops, Virtual, June 2020, pp. 229-237.
2. J. Redmon, S. Divvala, R. Girshick, A. Farhadi, “You only look once: Unified, realtime object detection,” In Proceedings of the IEEE Conf. Computer Vision and Pattern Recognition, Las Vegas, USA, June 2016, pp. 779-788.

A Study on Medical Computer-Aided Diagnosis for a Small Number of Labeled Training Data

Shingo Mabu[1]

[1]Department of Information Science and Engineering,
Yamaguchi University
Tokiwadai, 2-16-1, Ube 755-8611, Japan
[1]E-mail: mabu@yamaguchi-u.ac.jp

Digest

Machine learning, especially deep learning has been actively applied to computer-aided diagnosis (CAD) of medical images [1]. However, the typical problem of deep learning is that a large number of annotated (labeled) data is necessary to achieve high performance. Although it is important to build large-scale annotated databases of various organs and diseases for supervised learning, it is tough work for radiologists to give normal and abnormal labels to hundreds to thousands of images. Therefore, this research aimed to develop algorithms that can efficiently train deep neural networks based on 1) unsupervised learning without using labeled data, and 2) semi-supervised learning that makes use of a small number of labeled data and a large number of non-labeled data. In this study, two kinds of algorithms are introduced: 1) unsupervised learning using convolutional adversarial autoencoder (CAAE) for extracting image features [2], and 2) a semi-supervised Cycle GAN for image domain transformation [3]. These methods were applied to normal and abnormal opacity classification of diffuse lung diseases of chest CT images.

In the unsupervised learning, CAAE is used for feature extraction of the CT images. CAAE is an extension of an adversarial autoencoder (AAE) [4] using a convolutional neural network. Here, the feature extraction is carried out for region-of-interest (ROI) images that are extracted from the whole CT slices. Fig. 1 shows the flow of the method. After obtaining many ROI images, they are inputted to CAAE for feature extraction. Then, the extracted features are categorized by a clustering method, and finally, we obtain some clusters where the ROI images with similar features are in the same clusters.

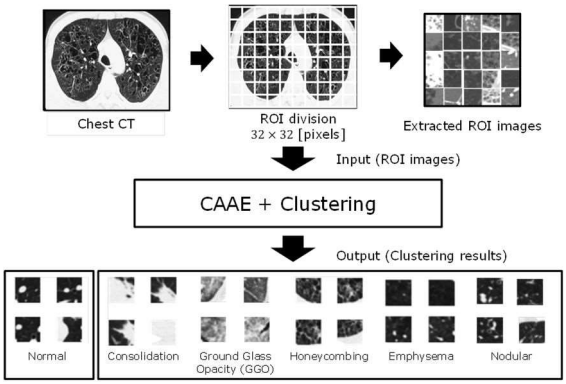

Fig. 1 Flow of ROI division, feature extraction by CAAE, and cluster generation.

In the semi-supervised learning, domain transformation of Cycle GAN is extended to semi-supervised learning. We used chest CT images taken by Yamaguchi University hospital (domain A) and Osaka University hospital (domain B). We aimed to train a classifier on domain A and apply it to the classification of domain B, and vice versa. However, the two hospitals use different CT devices, the features (appearance) of the CT images are different. In this case, one of the solutions to normalize the image features is applying Cycle GAN that can transform images between two domains. However, since Cycle GAN is trained in an unsupervised manner, it does not always transform to the images suitable for the opacity classification. To overcome this problem, we used a small number of labeled images to effectively transform images keeping the important features for classification.

From the experimental results, it was clarified that 1) the unsupervised learning with CAAE shows better clustering ability than the standard convolutional autoencoder (CAE) and 2) the semi-supervised learning of Cycle GAN can transform images so that they can be classified better than those transformed by the standard Cycle GAN.

References

1. H.C. Shin, H.R. Roth, M. Gao, L. Lu, Z. Xu, I. Nogue, J. Yao, D. Mollura, R.M. Summers, “Deep convolutional neural networks for computer-aided detection: CNN architectures, dataset characteristics and transfer learning”, IEEE transactions on medical imaging, vol. 35, no. 5, pp. 1285-1298, 2016
2. Y. Mitsukawa, S. Mabu, T. Kuremoto and S. Kido, “An Unsupervised Opacity Classification System for Chest CT images Using Convolutional Adversarial Autoencoder”, SICE SSI 2020, pp. 328-333, 2020 (in Japanese)
3. M. Miyake, S. Mabu, S. Kido, T. Kuremoto, “Domain Transformation of Chest CT Images Using Semi-Supervised Cycle GAN for Opacity Classification of Diffuse Lung Diseases”, Proc. of the 2021 International Conference on Artificial Life and Robotics, pp. 490–495, 2021
4. A. Makhzani, J. Shlens, N. Jaitly, I. Goodfellow and B. Frey, “Adversarial Autoencoders”, arXiv:1511.05644, 2016

Low Cost Simple Look-up Table based PMSM Drive Considering DC-link Voltage Variation

Jung-Hyo Lee[1]

[1]Department of Electrical Engineering, Kunsan National University
Daehak-ro 558 ,Gunsan, Korea
[1]E-mail: jhlee82@kunsan.ac.kr

Digest

This paper proposes a permanent magnet synchronous machine (PMSM) torque control method considering a DC-link voltage variation that can be utilized in a low cost DSP. For PMSM drives used in industrial applications, a two-dimensional look-up table (2D-LUT) is widely as a current reference owing to its stability and robust torque control performance. In general, a 2D-LUT is established using a flux-torque table to overcome the variation in DC-link voltage. However, this method requires a flux estimator for estimating the instantaneous flux, which is defined as a division of the operating speed used to obtain the flux data. Therefore, to obtain the operating flux, a variable division calculation or complex controller is used, which can be difficult to process through a low cost digital signal processor. In this paper, a novel look-up-table based control method that utilizes the newly established speed-torque 2D-LUT is proposed. This 2D-LUT inherently implements data on the d-/q-axis currents throughout the operating regions, not only the speed and torque, but also the DC-link voltage variation. The proposed method was verified through an experiment on the torque control a variation in the DC-link voltage.

Fig. 1 shows conventional 2D-LUT based PMSM control methods. The method of Fig.1(a) uses speed-torque input, therefore, it can not reflect DC-link voltage variation. The control method of Fig.1(b) can reflect DC-link voltage variation due to flux estimator, however, it needs comparatively complex procedure to obtain motor flux.

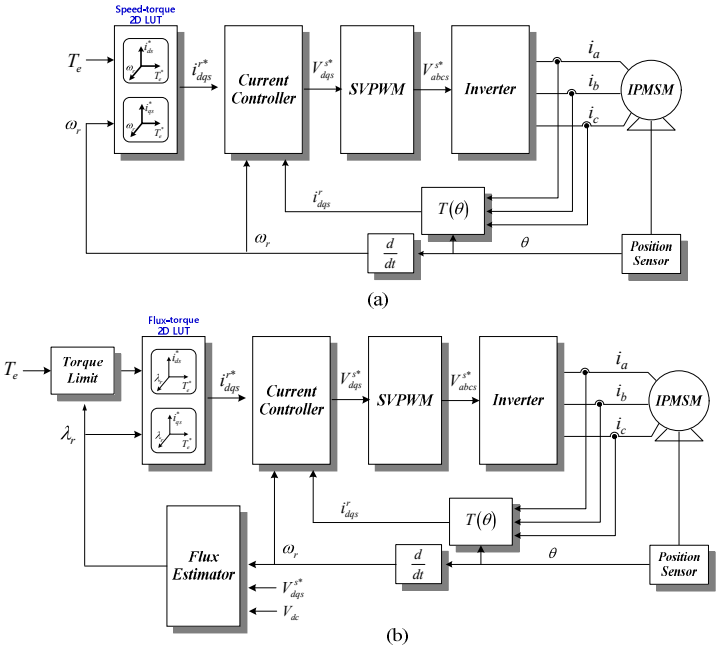

Fig. 1 LUT-based current reference controller: (a) speed-torque 2D-LUT based controller and (b) flux-torque 2D-LUT based controller.

Fig.2 shows proposed control method which can reflect DC-link voltage variation. It only uses voltage feedback controller to reflect input voltage indirectly. However, flux-torque 2D-LUT is needed to generate suitable dq-axis currents references, conventional speed-torque 2D-LUT can not use anymore. To solve this problem, we establish speed-torque 2D-LUT which has dq-axis currents data of the higher speed than practical maximum speed.

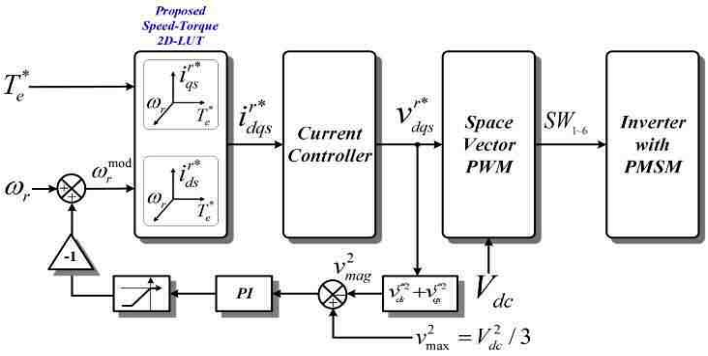

Fig. 2 Proposed speed-torque 2D-LUT based control method.

Based on this, Fig. 3 and 4 show dq-axis currents are varied with DC-link voltage, however, generated torque is constantly sustained with proposed control method.

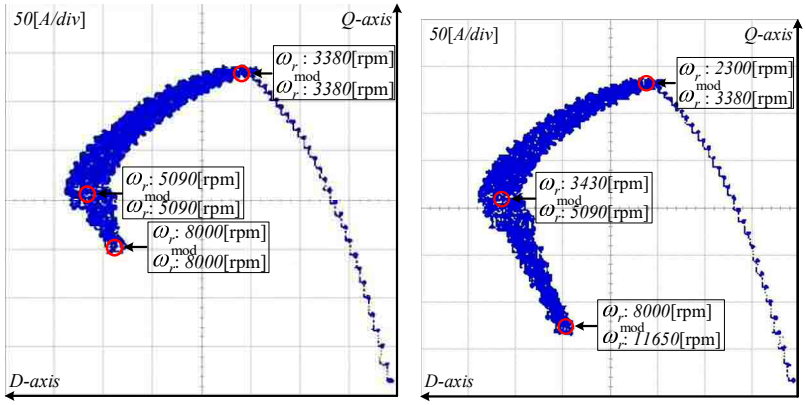

Fig. 3 dq-axis currents: (a) DC-link voltage 380V and (b) DC-link voltage 260V

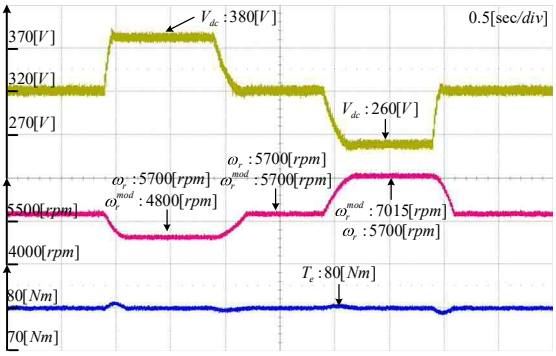

Fig. 4 Experimental results of variable DC-link voltage.

References

1. B. Cheng, Tesch, T.R., “Torque feedforward control technique for permanent-magnet synchronous motors,” IEEE-Trans. Ind. Elect., vol. 57, no. 3, pp. 969–974, Mar. 2010
2. E. Trancho, E. Ibarra, A. Arias, I. Kortabarria, J. Jurgens, L. Marengo, A. Fricasse, and J. Gragger, “PM-assisted synchronous reluctance machine flux weakening control for EV and HEV applications,” IEEE-Trans. Ind. Elect., vol. 65, no. 4, pp. 2986–2995, April 2018.

On Dual System Representation And Prediction Method for Data-Driven Estimation

Ryosuke Adachi[1] and Yuji Wakasa[1]

[1]Department of Electrical and Electronic Engineering, Yamaguchi University,
Tokiwadai, 2-16-1, Ube 755-8611, Japan
E-mail: r-adachi@yamaguchi-u.ac.jp

Digest

This paper addresses an observer-design method only using data. Usually, the observer requires a mathematical model of a system for a prediction of states and a calculation of an observer gain. As an alternative to the model-based prediction, the proposed predictor calculates the states using a linear combination of the given data. To design the observer gain, the data which represent dual systems are derived from the data which represents the original system. Linear matrix inequality that depends on data of the dual system provides the observer gains.

Consider the following linear time invariant system

$$x[k+1] = Ax[k] + Bu[k]\,,\ y[k] = Cx[k] + Du[k] \tag{1}$$

where, $x[k] \in \mathbb{R}^n$ is a state, $u[k] \in \mathbb{R}^m$ is an input, $y[k] \in \mathbb{R}^l$ is an output, $A \in \mathbb{R}^{n\times n}$, $B \in \mathbb{R}^{n\times m}$, $C \in \mathbb{R}^{l\times n}$ and $D \in \mathbb{R}^{l\times m}$. Let us define an experimental data of system (1) over $[0, T-1]$ as $\mathcal{D} := (\mathcal{U}, \mathcal{X}_-, \mathcal{X}_+, \mathcal{Y})$, where

$$\begin{aligned} &,\mathcal{U} := [u_d[0], \ldots, u_d[T-2]]\,, \mathcal{Y} := [y_d[0], \ldots, y_d[T-2]]\,, \\ &\mathcal{X}_- := [x_d[0], \ldots, x_d[T-2]]\,, \mathcal{Y}_+ := [x_d[1], \ldots, x_d[T-1]]\,. \end{aligned}$$

Dataset $\mathcal{D}$ indicates that state $\mathcal{X}_+$ and output $\mathcal{Y}$ are measured from an experiment when input $\mathcal{U}$ is applied to system (1) with state $\mathcal{X}_-$.

We utilize the data-riven predictor proposed in [1, 2] to simulate system (1). Let us find $\alpha[k] \in \mathbb{R}^{T-2}$ which satisfies

$$\begin{pmatrix} \hat{x}[k] \\ u[k] \end{pmatrix} = \begin{pmatrix} \mathcal{X}_- \\ \mathcal{U} \end{pmatrix} \alpha[k] \tag{2}$$

Then, next state $\bar{x}[k]$ and prediction of output $\bar{y}[k]$ can be calculated as

$$\begin{pmatrix} \bar{x}[k] \\ \bar{y}[k] \end{pmatrix} = \begin{pmatrix} \mathcal{X}_+ \\ \mathcal{Y} \end{pmatrix} \alpha[k]. \tag{3}$$

The dataset which represents a dual system of (1) can be expressed by

$$\begin{pmatrix} \mathrm{X}_+ \\ \mathrm{Y} \end{pmatrix} = \begin{pmatrix} \mathcal{X}_-^\top & \mathcal{U}^\top \end{pmatrix}^\dagger, \begin{pmatrix} \mathrm{X}_- \\ \mathrm{U} \end{pmatrix} = \begin{pmatrix} \mathcal{X}_+^\top & \mathcal{Y}^\top \end{pmatrix}^\dagger. \tag{4}$$

Thus the following gain stabilizes estimation error $e[k] = x[k] - \hat{x}[k]$:

$$L^\top = \mathrm{U}Q(\mathrm{X}_- Q)^{-1}, \tag{5}$$

where Q satisfies

$$\begin{pmatrix} \mathrm{X}_- Q & \mathrm{X}_+ Q \\ Q^\top \mathrm{X}_+^\top & \mathrm{X}_- Q \end{pmatrix} \succ 0. \tag{6}$$

This paper proposes the observer based on data-driven prediction and gain-design using duality. Based on the rank condition of data, data-driven predictor calculates output using a linear combination of the given data. To design the observer gains using only data, we calculate new data set which represents dual systems of the original ones. Based on the data which represent dual systems, we can calculate observer gain from linear matrix inequality.

References

[1] J. Berberich and F. Allgöwer, "A trajectory-based framework for data-driven system analysis and control," in *2020 European Control Conference (ECC)*. IEEE, 2020, pp. 1365–1370.

[2] C. De Persis and P. Tesi, "Formulas for data-driven control: Stabilization, optimality, and robustness," *IEEE Transactions on Automatic Control*, vol. 65, no. 3, pp. 909–924, 2019.

Student Poster Presentations

Grafted Polymer Chain-introduced Monolithic Silica Columns for Separation of Vaccine Virus

Junghu Lee
(Yamaguchi University, Japan)

1. Background

Adeno-associated virus(AAV) vectors vaccines

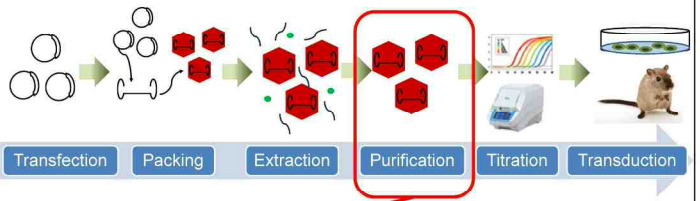

AAV Purification by chromatography*1

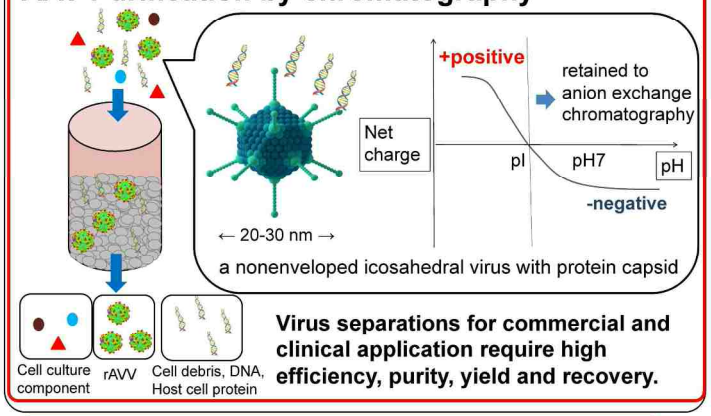

Virus separations for commercial and clinical application require high efficiency, purity, yield and recovery.

2. Meso-porous Silica Monolithic Column*2

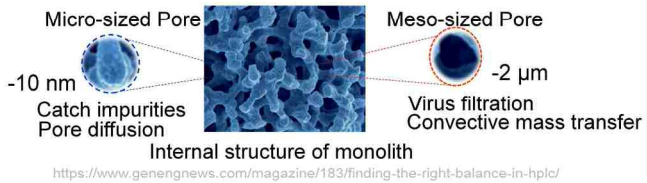

https://www.genengnews.com/magazine/183/finding-the-right-balance-in-hplc/

- Convective flow through the meso-sized pore realize high-speed processing of virus at low pressure.
- Micro-sized pores can provide the surface for adsorption, catch the target impurities, HCPs and DNAs.
- However, the binding capacity are limited inside micro-sized pore due to the low pore diffusion and interaction.

3. Research Objectives

- Introduce grafted polymer chains at monolithic pore to achieve the higher capacity of DNA and proteins*3.
- Evaluate performance for prepared columns(Peak conductivity, HETP; Height Equivalent to a Theoretical Plate, Resolution)

4. Introduce Polymer Chains & Evaluation

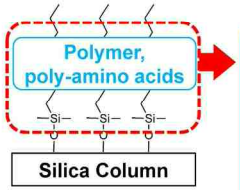

Larger Surface Area 😀
Low Pressure 😀

Prepared Columns

Ligand	Length	Column No.
Poly-lysine	short	#1
	middle	#2
	long	#3
Poly amino acid	middle	#4

① DNA 20T + TBS 100 μL
② DNA (3T – 70T) + TBS 100 μL — **DNA model**
③ 2 mg/mL BSA aq. — **Host cell protein model**

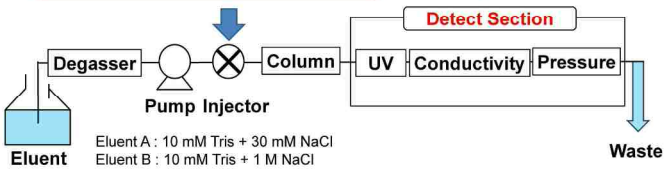

5. Experimental Results, DNA

① DNA 20T

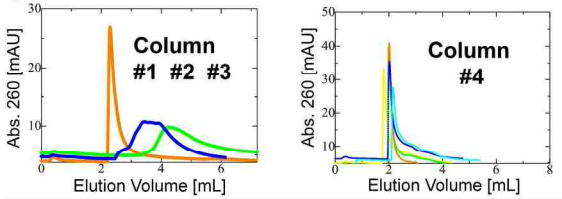

Ligand	Length	Peak cond. of poly 20T [mS/cm]
Poly-lysine I	#1 short	50.7
	#2 middle	78.8
	#3 long	76.6
Poly amino acid II	#4 middle	44.9
DEAE(conventional)	-	50.3

② DNA (3T – 70T)

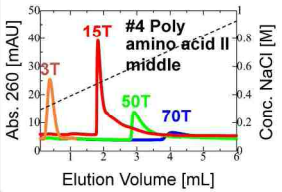

Sample	Peak cond. [mS/cm]	
	Ligand I*	Ligand II*
3T	4.4	4.4
15T	62.2	36.7
20T	78.8	44.9
50T	Over 150	70.4
70T	Over 150	79.8

(*Length: middle)

6. Experimental Results, proteins

③ BSA (protein model)

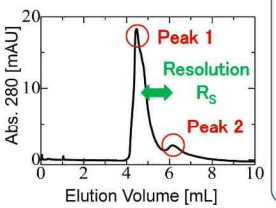

Column performance factors

$$HETP = \frac{Z}{N} = Z \times (\frac{\sigma_V}{V_R})^2 = Z \times \frac{(W_V/V_R)^2}{16}$$

$$R_S = \frac{V_{R2} - V_{R1}}{\frac{1}{2}(W_1 + W_2)}$$

(Z : Column length, V_R : Elution Volume, W : Peak width)

Column performance evaluation using BSA

Column	#1		#2		#3		#4	
HETP x 10^{-2} cm^{-1}	1.11	0.82	1.20	1.36	1.06	1.32	1.38	0.91
Resolution R_S	0.86		0.81		0.72		0.87	

7. Conclusions

- Polymers have been successfully introduced into columns.
- New grafted polymer chain-introduced monolithic columns (poly-lysine: #2 middle, #3 long) have powerful interaction capability compared to conventional monolithic columns.
- New columns also have good performance(HETP, R_S).

1. E. Burova and E Ioffe, *Gene Therapy* **12**, S5–S17, (2005). 2. T. Amatani, *et. al.*, *Chem. Mater.*, **17**, 8, 2114–2119, (2005). 3. C.-S. Chen *et. al.*, *J. Chromatogr. A*, 1629, 461495, (2020).

A Numerical Study on the Wave Characteristics Generated by Double Flap type

YAN KAICHENG

(Kunsan National University)

1. Research Background

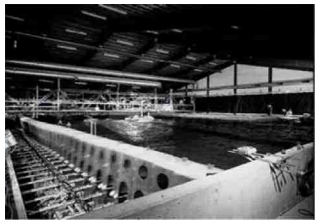

In the field of naval architecture and ocean engineering, nu
erical simulation and model test are two main approaches t
investigate the wave-structure interaction problems.

2. Induction Numerical Calculation Condition

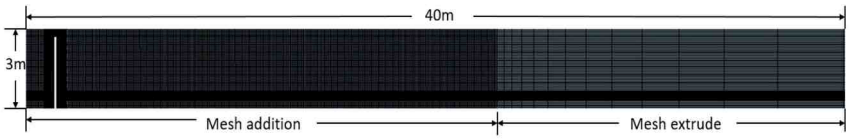

Dimensions of numerical wave-making tank

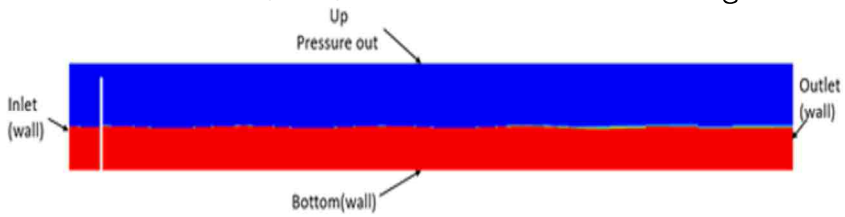

The definition of boundary conditions

3. Research Objectives

Comparing the wave heights of the Piston-type wavemaker and Flap-type wavemaker and Double-Flap type wavemaker obtained in the three-dimensional model.

4.Numerical Tank calculation

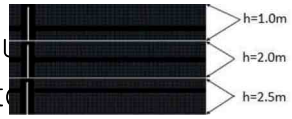

Piston type wavemaker

Flap type wavemaker

Double-flap type wavemaker

5. Numerical Resultsc

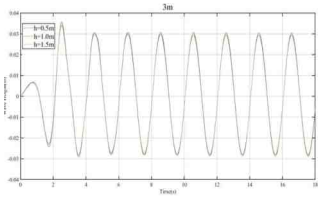

Piston type wave curve of different water depth at 3m

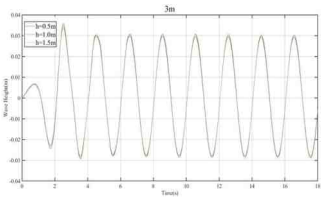

Flap type wave curve of different water depth at 3m

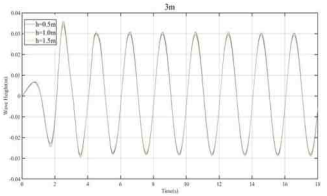

Double-flap type wave curve of different water depth at 3m

6. Condusitions

1. The wave-making effect of the Piston-type wavemaker is the worst in the shallow water.
2. Under the circumstances, the effect of Double-Flap type wavemaker is the best

References

[1] William Finnegan, Jamie Goggin, 2015, Linear irregular wave generation in a Numerical wave tank, Applied Ocean Research, pp 188-200

[2] Pal schmitt, Christian Windt, Josh Davidson, 2019, The Efficient Application of an Impulse Source Wavemaker to CFD Simulations MDPI,2019.7.71

Effect of Martensite Low Alloy Steel on Hydrogen Sensitivity

T. Ishibashi ,T. Oda , D. Hayashi , R. Fukuoka and Arnaud. Macadre

(Yamaguchi University, Japan)

1.Research Background

Utilization of Hydrogen energy

Concerns about resource depletion,
The use of **hydrogen energy** is currently attracting attention.

However, the infrastructure development of hydrogen stations has been delayed…

Cause of infrastructure development

An example is material selection considering **hydrogen brittleness**

SUS304

SUS304,which has excellent corrosion resistance ,is used as a material ,but the cost is very high

Therefore, the low-cost…

Considering chrome molybdenum steel as an alternative material

2.Introduction of chrome molybdenum steel

Feature of chrome molybdenum steel

- Excellent hardenability
- High resistance to tempering
- Relatively cheap due to low Ni

Material	price [dollar/ton]
SUS304	59000
SCM435	15000

About 4 times cheaper than SUS304

3.Research Objective

Investigation of hydrogen brittle sensitivity by tensile test

In this study, the sensitivity of hydrogen is investigated by conducting a **tensile test** on a test piece (SCM415,SCM440) whose hardness has been changed by heat treatment.

4.Research conditions and results

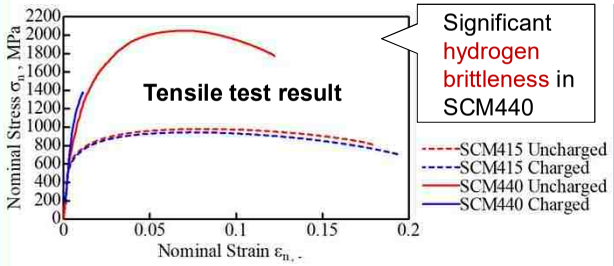

Significant hydrogen brittleness in SCM440

Heat treatment
Quenching **1h 900℃** oil cooling
Tempering **1h 160℃** air cooling
Hydrogen charging
NaOH 500ml ,Current 0.01A
Current density 111A/m^2 ,72h
Tensile test
Cross head speed 0.5mm/min

Uses dumbbell-shaped test piece

Fracture surface observation result

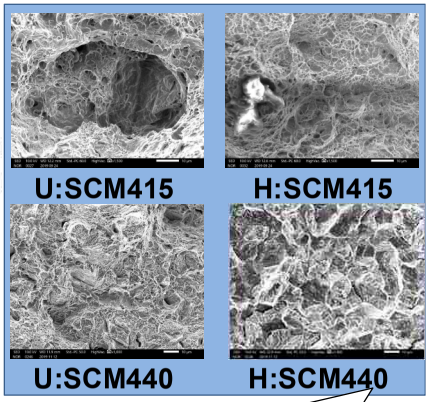

Grain boundary destruction is seen after hydrogen charging in SCM440

5.Conclusions

It can be seen that **the higher the strength** of the material the more susceptible it is to hydrogen embrittlement

Numerical Study of the Free Decay Test for the Semi-submersible Structures of Floating Offshore Wind Turbines

Sebum Oh

(Kunsan National University, Republic of Korea)

1. Research Background

OC5 form(Yin Zhang, et al 2018)

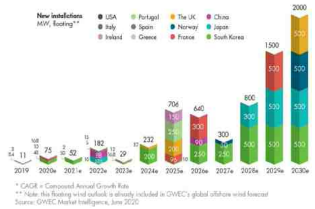

-GWEC market Intelligence

- problem & Policy

1. Carbon emission Regulation

- Recycle Engery Spotlight

1. Various Energy..

Wind Energy

Typically

Civil, land, condition problem

- Floating offshore wind turbine

disturbance reduction

- Optimal form(CFD)

caused by reduce motion

2. Test Form

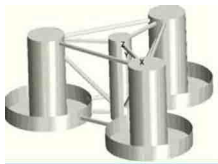

Principal Dimension	Value
Mass	13898856kg
Draft	24.01m
CM below SWL	5.79m
Skirt Diameter	-
Center Column Diameter	9.205064704m
Side Column Diameter	14.7050647m

Form 1(w/o plate)

Principal Dimension	Value
Mass	13898856kg
Draft	24m
CM below SWL	5.8m
Skirt Diameter	34.3132747m
Center Column Diameter	9.205064704m
Side Column Diameter	14.7050647m

Form 2(hollow plate)

Principal Dimension	Value
Mass	13898856kg
Draft	24m
CM below SWL	5.8m
Skirt Diameter	34.3113274 7m
Center Column Diameter	9.205064704m
Side Column Diameter	14.7050647m

Form 3(up and down plate)

3. Research objective

- Optimal substructure form considering reduction motion to the energy supply process of floating offshore wind power generators according to Free Decay test the semi-submersible structure(using CFD)

4. Simulation

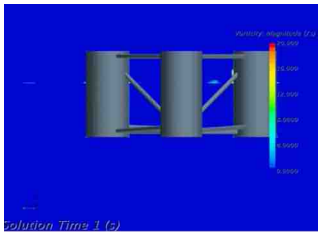

Form 1(w/o plate)

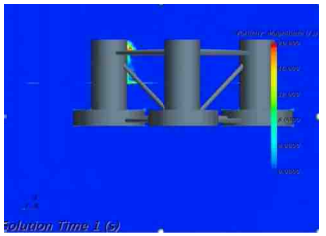

Form 2(hollow plate)

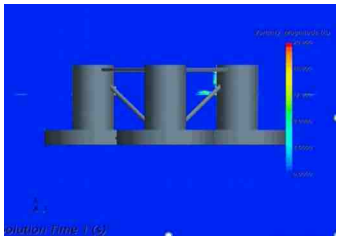

Form 3(up and down plate)

- Each type of simulation using CFD(STAR CCM+).

5. Test Result

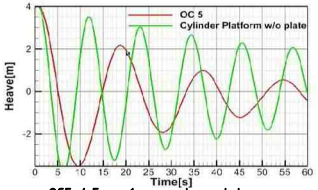

OC5 / Form 1 comparison plot

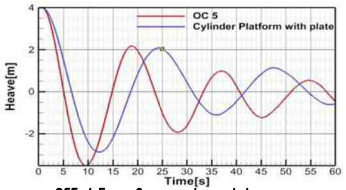

OC5 / Form 2 comparison plot

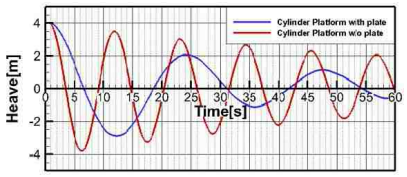

OC5 / Form 3 comparison plot

- Separation of flow due to vortex generation and promotion of motion reduction effect due to vortex shedding.

6. Conclusions

- Fluid viscosity strongly affects the total damping of the floating platform with heave plate.
- The attenuation rate of heave free decay motion in the first period is about 38.3% in OC5, and the difference of the Cylinder Platform with plate and Cylinder Platform without plate are 14.3% and 46.1% which illustrates that the area of heave plate is strongly related to the attenuation rate in heave DOF.

7. References

- [1] Sewan Park, kyong-Hwan kim, and keyyong hong "Conceptual Design of motion Reduction Device for Floating Wave-Offshore Wind hybrid power Generation Platform." Journal of Ocean Engineering and Technology pp 9-20, February, 2018.
- [2] Yin Zhang and Bumsuk kim " A Fully Coupled Compuational Fluid Dynamics Method for Analysis of Semi-submersible Floating Offshore Wind Turbines Under Wind-Wave Excitation Conditions Based on OC5 Data." Jeju University, September 2018.

Iron and Manganese Surface Treatment on Anode Electrodes in Plant Microbial Fuel Cells for Improved Bio-Electricity Generation

S. Uramoto, M. Azizul Moqsud

Division of Construction and Environmental Engineering, Yamaguchi University, Japan

1. Introduction of PMFCs

Plant Microbial Fuel Cells (PMFCs)

- Components: Plants, soil, and Bacteria
- Function: To generate Bio-electricity
- Advantages: Clean and Sustainable

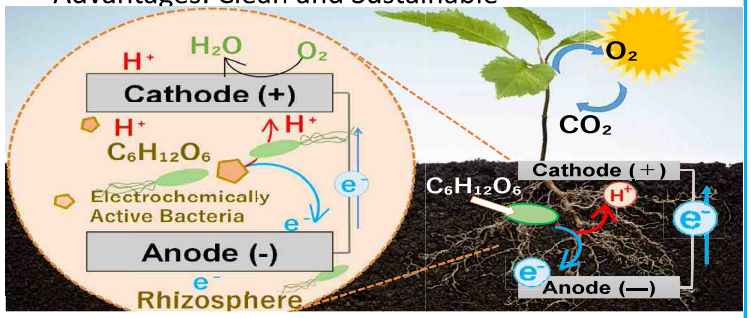

Fig. 1 Diagram of Plant Microbial Fuel Cells

2. Research Background and Objectives

The biggest problem is low power generation in non-aquatic plants' PMFCs

Table 1. PMFCs researches in different plants species

Plants	Plant type	Power (mW/m²)
Glyceria maxima	Aquatic	67.0
Lemnaminuta	Aquatic	380.0
Spartina anglica	Aquatic plant	240.0
Paddy rice plant	Aquatic plant	39.2
Sedum hydridum	Non-aquatic	0.09
Sedum rupestre	Non-aquatic	0.02

To improve electricity production in non-aquatic plant

Mn × Fe

- Biocompatibility
- Bacteria adhesion
- High conductivity

3. Materials and Methods

Fig. 2 Anode's chemical treatment process

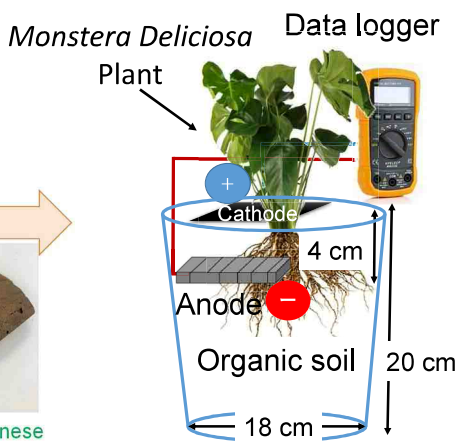

Fig. 3 PMFC design

4. Results

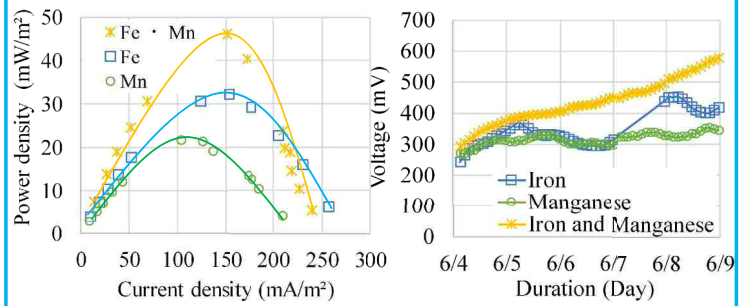

Fig. 4 Power densities

Fig. 5 Voltage variation

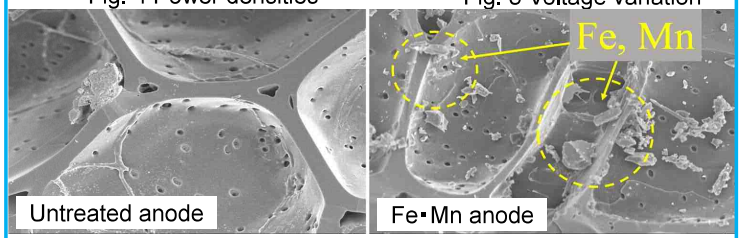

Fig. 6 Optical analysis of anode surface by using SEM

5. Conclusion

- Bio electricity was improved with Fe and Mn even with non aquatic plant
- Highest power was 46 mW/m² 130%, and 220% improved compared to Fe treatment, and Mn treatment

6. Reference

- Rukhsar Shaikha, Afshan Rizvia , Marzuqa Quraishia , Soumya Panditb, Abhilasha Singh Mathuriyab , Piyush Kumar Guptab , Joginder Singhc , Ram Prasad., "Bioelectricity production using plant-microbial fuel cell: Present state of art", South African Journal of Botany,pp1-16,2020
- Moqsud,M.A J. Yoshitake, Q.S. Bushra, M. Hyodo, K. Omine, David Strik., Microbial fuel cell (MFC) for bioelectricity generation from organic wastes. Waste management, Vol 36, 2015, pp 63-69

Structural Design and Analysis of Gear Pump for Mechanical System

Yonggyu Lee
(KUNSAN NATIONAL UNIVERSITY. Republic of Korea)

1. Theory of Gear Design

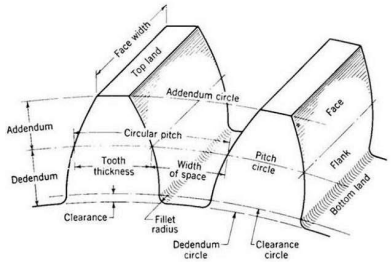

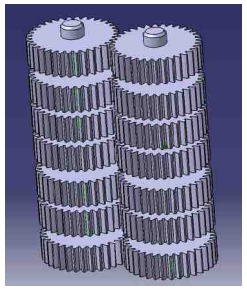

	Size(mm)
Number of teeth	34
Normal Module(M)	2
Angle Pressure	20°
Face Width(mm)	20
Addendum	1M
Dedendum	1.25M

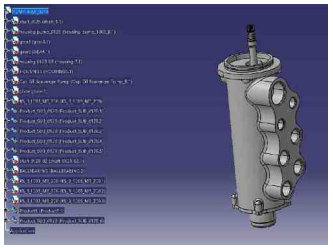

Hydraulic driving is widely used as a means of realizing large-scale and automatic machinery in various industries.

3. Analysis Result

Time[s]	Minimum[mm]	Maximum[mm]
1.1755e-038	0	1.5888e-014
1.e-004	2.2204e-016	6.0485
2.0002e-004	2.2204e-016	11.091
3.e-004	2.2204e-016	15.69
3.85e-004	2.2204e-016	19.692

Time[s]	Minimum[MPa]	Maximum[MPa]
1.1755e-038	0	0
1.e-004	0	4875.4
2.0002e-004	0	6365.8
3.e-004	0	14487
3.85e-004	0	22266

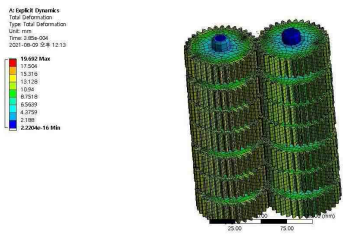

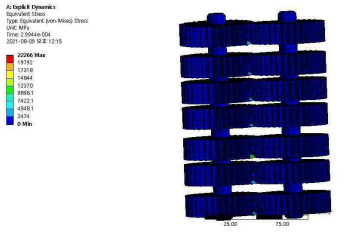

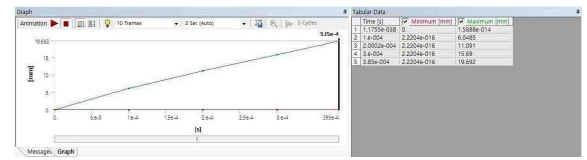

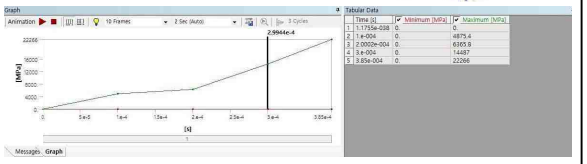

2. Gear Analysis using ANSYS Software

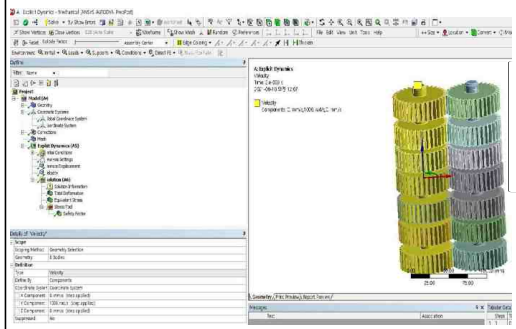

Analysis System: Explicit Dynamics

Coordinate System: Cylindrical Type

Principal Axis: Z(Axis), Global X Axis

Boundary conditions: Velocity

Velocity: 0(X),1000rad/s(Y),0(Z)

Boundary Conditions: Remote Displacement

Type: 0(All, Component, Rotation)

4. Conclusions

- The structural analysis result using ANSYS software was presented the results of the values of total deformation, equivalent stress, and safety factor.
- Increasing the size of the module during gear design naturally reduces the number of gears, thus increasing the life and yield stress values of the gears.

5. References

[1] Jang-pyo Hong, "Mechanical Element Design Point", Kyobo Bookstore, p440-571.
[2] Seung-il Ahn. "A Study on the Design of External Gear Pump." Korea Master's Degree Paper Changwon University Graduate School of Industrial Information, 2007. Gyeongsangnam-do.
[3] Jae-yeon Jung, Chul-ho, and Chang-gu Jung (1995). A Study on the Characteristics of Hydraulic Gear Pump (see Step 2) (A Study on the Characters of Hydraulic Gear Pump (2nd Report). Spring and Autumn Conference of the Korean Mechanical Society, 137-142.

Method for Animating Water-Flow in an Illustration

Yusuke Kawazu and Katsumi Tadamura
(Yamaguchi University, Japan)

1.Introduction

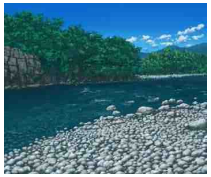

A still image such as a landscape picture or an illustration sometimes includes portions that essentially have motion.
→It is not easy to express this motion.

Conventional method: Use of fragmented video material
[1] Animating Pictures of Water Scenes using Video Retrieval, M.Okabe, et al., 2018
[2] Development of a Support Tool for Creating Water-Flow Animation from a Single Image, S. Kinuta, et al.,2019
→Quite large difference between the textures of the hand-drawn portion and the animated portion appears because the video fragments are used directly.

We need a method that enables us to animate water-flow in an illustration while keeping its texture.

We propose a method for animating a water-flow portion in an illustration without losing its hand-drawn texture.

2.Basic Ideas

Input and output data:

Input data
- One water-flow video material
- An illustration (the water-flow in it is unidirectional)

Output data
-The animation created by synthesizing the motion information into the water-flow portion (Synthesized motion information is cut out from a fixed area of the video)

The features of the proposed method:
It does not request complicated operation to the user.
The user need not take into account matching the color between the water surface in the illustration and that of synthesized video.

Constraints:
-Only one water-flow is animated in an illustration.
-The texture of the water-flow depends on the synthesized video material.

Video material example

Illustration example

3.Outline of the Method

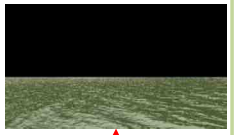

Read illustration and video material

Color reduction processing

Specify the water-flow direction

Cut out the water-flow portion of the illustration

Specify and cut out a fixed area of the video material

Synthesize the motion with the illustration

Output water-flow video

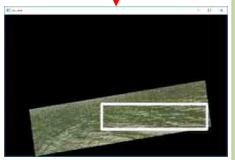

4.Examples and Conclusion

We proposed a method for animating a water-flow portion in an illustration without losing its hand-drawn texture and its usefulness was confirmed through applying to some examples.

Future challenge will involve developing a method to animate a water-flow with multiple stream-directions in an illustration by synthesizing multiple water-flow videos.

Performance Analysis of Consequent Pole Vernier Machine for MW Scale Wind Power Generator

Abdur Rehman and Byungtaek Kim

(Kunsan National University, Republic of Korea)

1) Research Background

- **Direct drive** (DD) **topology** (no gear box) is **more suitable** for **offshore wind power generation**,

$$P_{mech.} = \omega\tau$$

- **DD generator involves** higher **raw material**, **manufacturing** and **installation concerns**,
- So, for **DD system** it is **necessary** to use **high torque density generator** (lower size)
- **SPM Vernier** is **famous** due to its **higher torque density** [1],
- **Consequent pole (CP) rotor** has **interesting advantages** when **used** with **SPM Vernier machine** [2].

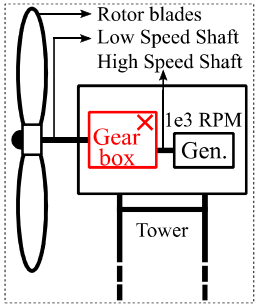

2) Design Process

- Two **CP-PM vernier prototypes** (**10 MW**) are **designed** with **different gear ratios**, and **their performance** is **compared with** a **10 MW DD SPM generator** by **NREL.**

$$P_{mech.} = \underbrace{(\omega_m K_w)}_{1}\underbrace{(K_s F_{g1})}_{2}\underbrace{(D_g^2 l_{stk})}_{3}\underbrace{(P_{g0} + (0.5 P_{g1} G_r))}_{4}$$

$$G_r = \frac{Z_r}{p_{mod}}$$

- Following graph **helps** to **select** a **slot/pole combination**,

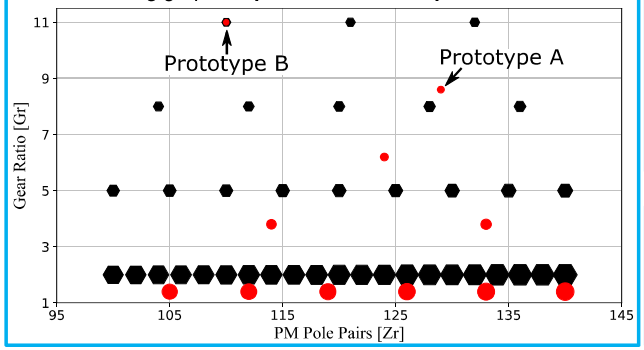

3) Analysis Model and FEM Results

- The **main design parameters** of the **two prototypes in comparison** with the **reference model** (**NREL**) are give in the following **table**,

Main Design Parameters	Reference Model	Prototype A ($G_r = 8.6$)	Prototype B ($G_r = 11$)
Air-gap diameter	10.3 m	7.7 m	7.0 m
Air-gap length	10.29 mm	7.7 mm	7.0 mm
Magnet thickness	39.5 mm	40 mm	45 mm
I_{max} at (K_s = 53.9 kA/m)	907 A	679 A	618 A
Rated Speed	8.76 rpm		
No. of Stator Slots	240	144	120
No. of PM Pole Pairs	100	129	110
Coils turns per phase	320		
PM Remanence	1.33 T		

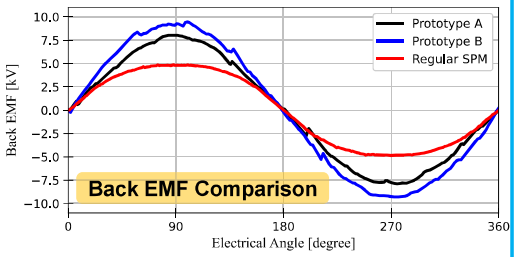

- Despite of **lower** D_g of prototypes, they have higher back EMF than SPMM,
- **Rotor teeth** is **severely saturated** and it will **limit** the **torque performance**
- To **see** the **saturation effects** the torque is calculated at k_{max} and 0.5 k_{max}.

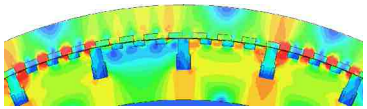

Prototype A ($G_r = 8.6$)

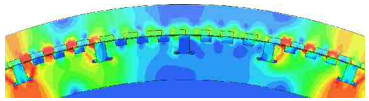

Prototype B ($G_r = 11$)

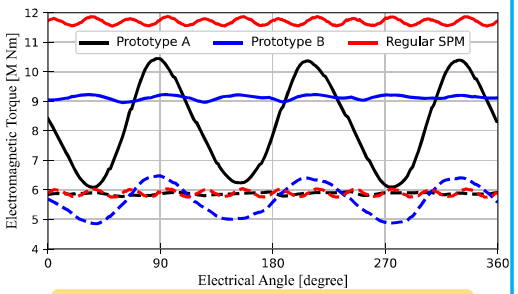

Comparison of Torque Characteristics

4) Conclusions

- ✓ The **calculation results shows** that **both** the **prototypes** with much **reduced magnet material** (due to **CP rotor**) and **up to 32 % less air-gap diameter** can produce the **same rated power.**
- ✓ Although, the **back EMF** of prototype A and B are **1.38** and **1.68 times higher than** that of **reference model** but the **torque value** is **less** than **expected**, and this is because of the **saturation effect.**
- ✓ The **saturation** has **effect** on the **power factor** however, for **both prototypes** it is around **20%** in comparison with **87 %** of reference model.

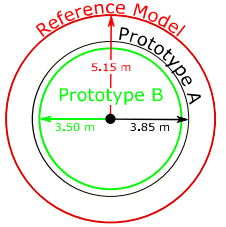

5) References

1. B. Kim, "Design method of a direct drive permanent magnet Vernier generator for a wind turbine system," IEEE Trans. Ind. Appl., vol. 55, no. 1, pp. 4665-7675, Jun. 2019.
2. A. Rehman, B. Kim, "Characteristics analysis of a consequent pole ferrite magnet vernier machine using novel equivalent magnetic circuit," IEEE J. Emerg. Sel. Topics Power Electronics.

Combination of high-temperature fermentation and membrane separation for bio-ethanol production

Y. Shimada, M. Yamada and I. Kumakiri

1.Background

Transportation is one of the large CO_2 emitting sectors[1]. Substituting fossil fuel by bio-fuels will reduce the CO_2 emission.

1) D.S. Sholl, R. P. Lively, Nature news, 532, 435, 2016

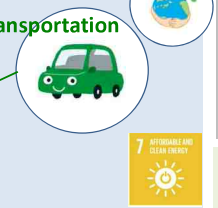

"High-temperature fermentation" (Agriculture Faculty, Yamaguchi Univ.)

Concentration process needs to be energy efficient.

2. Different processes to concentrate bio-ethanol

Conventional process (Distillation) **Membrane-based process**

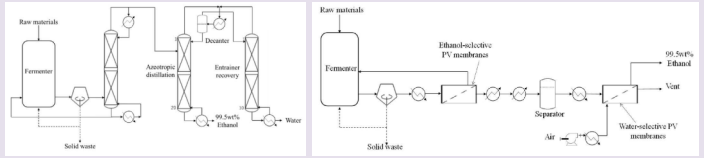

I. Kumakiri, *et al.* Process 9,1028,2021

Process Configuration	Energy Demand(W/kg-EtOH)		
	10 → 80wt% ethanol	80 → 99.5wt% ethanol	Total
Distillation+azeotropic distillation	**1804**	**2339**	**4142**
DIstillation+ dehydration membrane (commercialized process)	**1804**	**287**	**2091**
Ethanol-selective membrane + dehydration membrane	1199	**277**	**1480**

Application of membrane
saves 65% energy consumption

3.Reserch Objective

Investigate the influence of fermented solution on the ethanol-selective membrane properties.

4.Membrane synthesis

Molar composition of the synthesis solution
SiO_2:TPABr:NaOH:H_2O=1:0.05:0.08:75

Mullite support + seed crystals → **Hydrothermal synthesis (180℃,8h)**

MFI Membrane with tetrapropylammonium bromid (TPABr)

Calcination (500℃,20h)

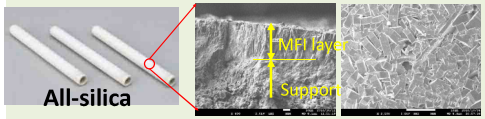

All-silica MFI Membrane | Cross Section | Surface

5.Separation tests (pervaporation, PV)

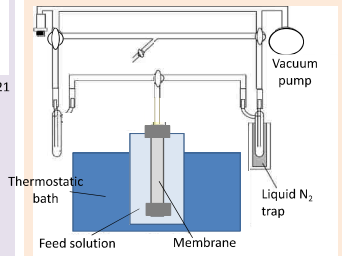

Feed solutions
- H_2O:EtOH/87:13wt%
- Fermented solution(FS) H_2O:EtOH/87:13wt% + small amount of organic acids, etc...

▪Flux $Q=\frac{W}{A \cdot t}$ [kg▪m^{-2}▪h^{-1}]
W: Permeate weight [kg],
A: Membrane area [m^2],
t: Collection time[h]

▪Separation factor $\alpha=\frac{(YA/YB)}{(XA/XB)}$ [–]
$X_{A(B)}$:Water (ethanol) weight fraction in the feed
$Y_{A(B)}$: Water (ethanol) weight fraction wt% in the permeate

6.Results

6.1 Separation of fermented solution (FS) at 75℃

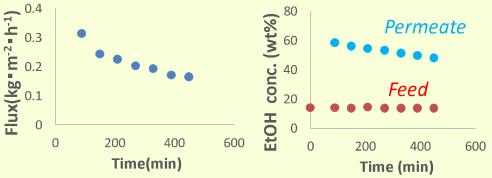

- MFI membrane concentrated ethanol in the FS.
- Both flux and selectivity decreased with time.

6.2 Separation of binary mixture at 75℃

Membrane conditions	Flux (kg·m^{-2}·h^{-1})	Separation factor (-)	Permeate EtOH conc. (wt%)
Fresh membrane	1.4	17	71
After treating FS	0.7	16	73
After heat treatment at 500℃	1.6	16	69

6.3 XRD after FS separation

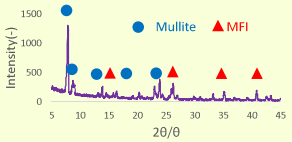

- Flux became about half to the fresh membrane after FS separation and recovered after heating.
- XRD showed no changes, suggesting robustness of the membrane.

7.Discussion

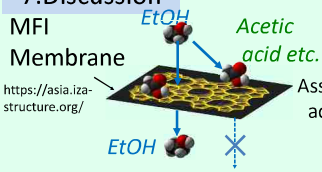

Why did flux decline and then come back by heating?

Assumption: Acetic/lactic acids etc. in the FS adsorbed to MFI membranes and plugged the zeolitic pores of ca. 0.5 nm.
→ Ethanol flux reduction ?

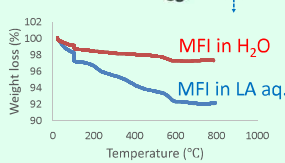

Thermogravimetry (TG) analyses showed larger weigh decrease when MFI powder was immersed in dilute lactic acid (LA) solution, suggesting LA adsorption to MFI.

8.Summary and prospects

All-silica MFI membranes concentrated ethanol in a fermented solution. However, both flux and separation properties were lower than in a binary mixture separation. Adsorption of organic acids may cause these reductions. Pre-treating the fermented solution and applying membrane surface modifications will be studied to improve the membrane performance.

Battery cell balancing unit for manufacturing industy

Hyeon-sik Kang,Se-dong Yang, Sung-ha Son, Jung-hyo Lee

(Kunsan University, Korea)

introduction

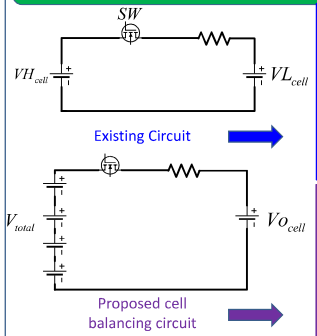

- One high cell voltage -> One low cell voltage
- Balancing time is long
- Switch on voltage Drop occurred
- Existence of voltage error between cells

- Balancing with full battery voltage
- Fast cell balancing with small voltage differences
- By default, a very small internal cell resistance causes a large current flow at turn-on

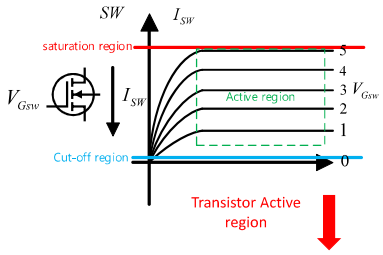

- Using switch active region to limit excessive currenst
- Current flowing through the switch varies with gate(base) voltage VGsw
- VGsw is applied between 0~5 V to adjust the magnitude of the current accordingly

Control Algorithm

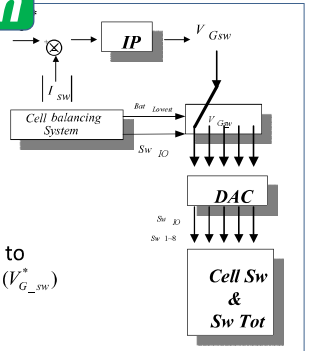

- Purpose of current limitation in battery cells through active area control
- $I^*$was selected as 1A and the active area voltage control command was generated through IP controller$(V^*_{G_sw})$
- Determining which switch the voltage command from the cell balancing system to which Bat_{lowest}information is to be applied $(V^*_{G\_sw})$
- Output via DAC

System Configuration

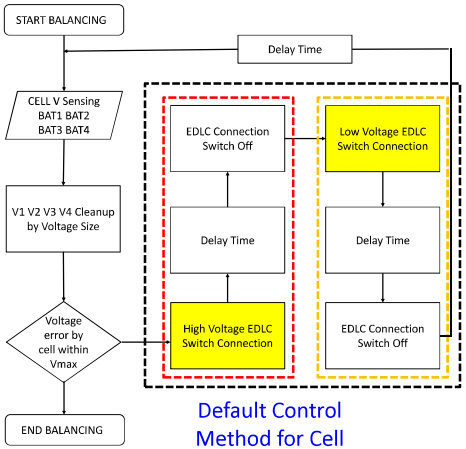

Default Control Method for Cell Balancing

MODE 1 : Charging the full voltage to the EDLC

MODE 2 : Transfer energy charged to EDLC to lowest cell

- Sensing voltage information from 4 batteries
- List in order of sensed voltage information size
- Full Voltage EDLC Charging
- EDLC Switch Off
- Lowest BAT connection
- EDLC Switch Off
- Perform the same action

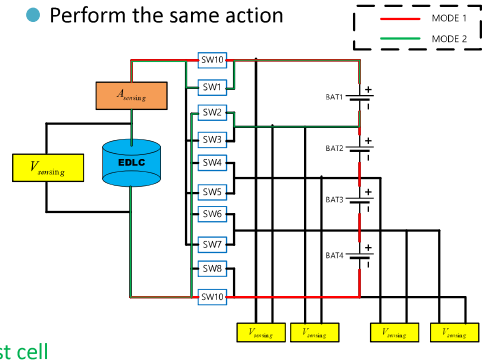

Current Pass by Cell Balancing Circuit Configuration and Control Method

Experimental Results

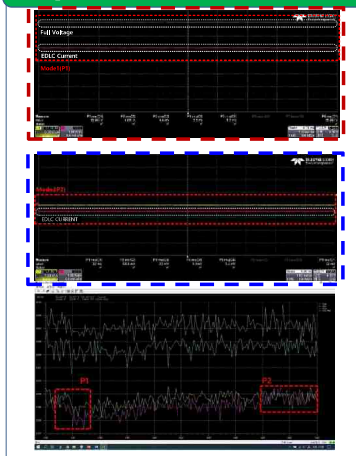

- Indicates the overall voltage EDLC state of charge, which is Mode1 operation
- Current limit due to full voltage charging is limited to 1A via IP controller
- The lowest battery cell in Mode 2 operation, charged in the EDLC, As the voltage is transmitted, it can be seen that reverse current flows.

Experimental set

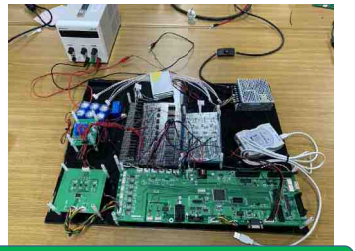

Conclusion

As a way to improve the shortcomings of cell balancing circuits, BJT's voltage-current characteristics were used to reduce balancing time and improve accuracy.

Reference

Seonwoo Jeon, Jae-Jung Yun, Sungwoo Bae. "Active Cell Balancing Circuit for Series-connected Battery Cells. " ICPE(ISPE) . (2015): 1182-1187.

Asif Hussain, Hakjun Lee, Seung-Ki Sul. "An Active Forward Fly-back Balancing Circuit for Series Connected Supercapacitors." The Korean Institute of Power Electronics . (2010): 228-229.

Fall Detection based on Autoencoder with Obrid-Sensor

T. Sunakawa, Y. Horikawa and S. Nakashima
Yamaguchi University, Japan

Research Background

Monitoring Sensors for the Elderly with Privacy Protection

684,000 individuals die from fall accident each year [1].

For protect from falling danger,
It is needed monitoring sensors in their private room.

Therefore, It is required 3 elements:

- **Privacy Protection**
- **Easy Installation**
- **Less Misclassification**

One-Dimensional Brightness Distribution Sensor (Obrid-Sensor)

Obrid-Sensor consists of Line-Sensor and Cylindrical Lens [2].

The line sensor is used such as scanners.

And the cylindrical lens integrates the brightness.

The sensor can detect Position, **State** from features like images but **No-Detail.**

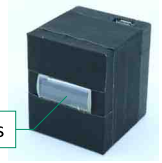

Obrid-Sensor

Standing State

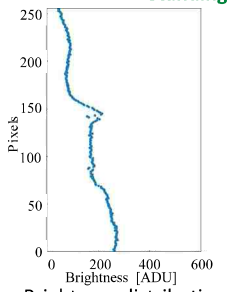

Brightness distribution


Camera image

Falling State

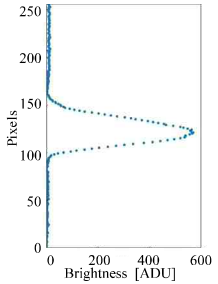

Brightness distribution


Camera image

Proposed Method

Detection based on Autoencoder

The model trains by standing data only and detect anomaly state.

If it obtains **standing** waveform, **reconstruction is successful**.

If it obtains **falling** waveform, **reconstruction is failed**.

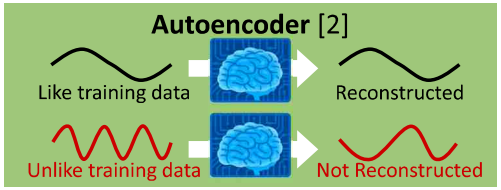

Convolution Layer

Ordinary autoencoders cannot learn the dependency of neurons in the same layer.

So, we added a convolutional layers for shift invariant.

Anomaly Score

We calculate Residuals Sum of Squared (RSS) as **Anomaly Score** from input date and reconstructed data.
If the score exceeds the threshold, it is classified as falling.

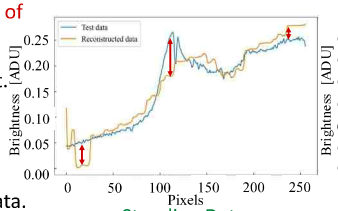

Standing Data
→**Low Anomaly Score**

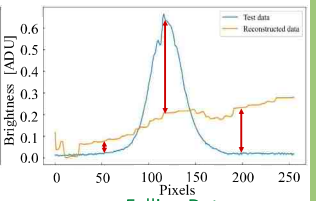

Falling Data
→**High Anomaly Score**

Experiment

Conditions

We prepared 450 standing data and set the threshold.

Standing Data	Falling Data	Total
450	0	450

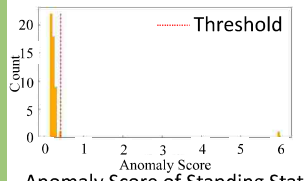

Anomaly Score of Standing State

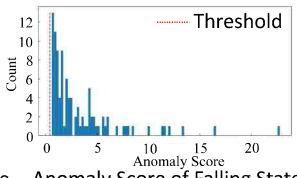

Anomaly Score of Falling State

Results

The results were validated on 150 test data.

		Output	
		Standing	Falling
State	Standing	48	2
	Falling	0	100

Accuracy [%]	Precision [%]	Recall [%]	F1 Score [%]
98.7	98.0	100.0	99.0

Easy Installation and **less misclassification**

Previous Research

Falling/Standing Detection based on Support Vector Machine (SVM)

The classification accuracy of SVM was high,
but it was difficult to prepare falling data to training.

Standing Data	Falling Data	Total
288	288	576

		Output	
		Standing	Falling
State	Standing	27	2
	Falling	0	29

Conclusion

- Detecting anomaly based on Autoencoder is proposed.
- The proposed method was more accurate than SVM and easier to install because it requires less training data.
- We are working on development more accurate classifier based on more advanced Autoencoder (VAE, etc.)

Reference

[1] Susan P. Baker, and Ann Hall Harvey : "Fall injuries in the elderly.", Clinics in Geriatric Medicine, Volume 1, Issue 3, pp. 501-512,1985

[2] J.K.Chow, Z.Su, et al : "Anomaly detection of defects on concrete structures with the convolutional autoencoder", Advanced Engineering Informatics, Volume 45, pp.101-105, 2020

Numerical simulation of a hazardous gas leakage accident in Saemangum industrial park

Lee Jaebeen[1)] *, Oh Seoungchan[1)] Jo Wanjae[1)] , Moon Jemin[1)] , Son Donghui[1)] , Joo Junghoon[1)] , Kim Seongbong[2)]

[1]Kunsan National University, [2] Korea Institute of Fusion Energy

1. Introduction

There are many companies using hazardous chemicals in Saemangum industrial park : hydrochloric acid, sulfuric acid, nitric acid, and ammonia.

Chemical related accidents occur every year about 80 cases nationwide, and also occur abroad. The most common accident types were leaks, followed by explosions and fires.

Assuming accidents caused by leak, we assessed potential damage area and the necessary evacuation time in the industrial park area by CFD-ACE+.

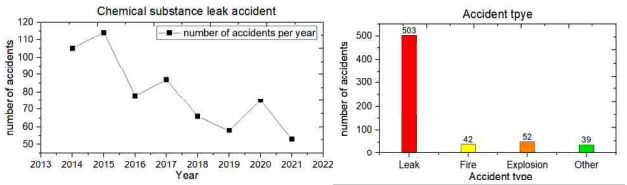

Figure1. number of chemicals accidents per year in Korea (ICIS) and type

2. Hazardous gas users in Saemangum

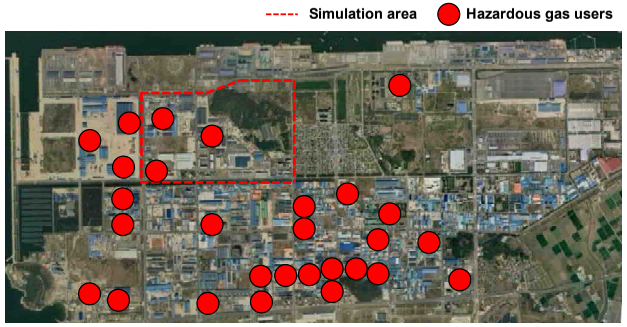

Figure2. Saemangum industrial park (Google map)

- Chemical handling company: Total 28 companies
- Amount of chemicals: 457,171 tons
- Chemical type: Hydrogen sulfide, Hydrogen chloride, Sodium hydroxide, hydrogen nitride etc.
- Accident status: 16 cases
- Accident type: leak 14 cases, explosion 2 cases

4. Simulation condition

- **Leak gas type: Hydrogen chloride (HCl)**
  - ✓ The dangers of HCl
    - Lethal dose 1,300 ppm 30 min / 3,000 ppm 5 min
    - Permit exposure limit: 5 ppm
    - Recommend exposure limit: 5 ppm
    - Immediately dangerous level to life or health: 50 ppm

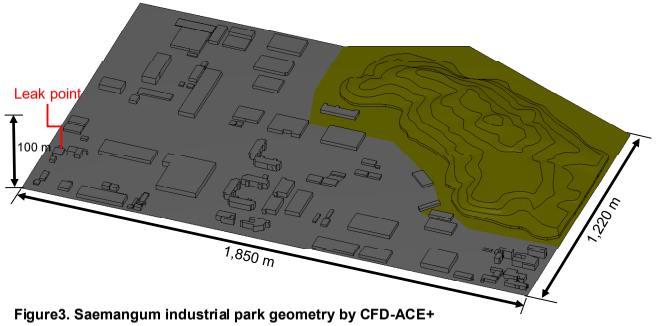

Figure3. Saemangum industrial park geometry by CFD-ACE+

	Value
Simulation area	2.1×10^6 m^2
Total cells	3,465,916 cells
state	1 atm, 27°C (Standard)
Wind condition	0 ~ 15 m/s (N2, O2)
Leak condition	1 m/s (HCl), 132 m^2
Simulation method	Transient, Parallel run 12 Core
Time step	1 sec (output: 30 iteration = 30 sec)

Table 1. Simulation conditions

4. Simulation result

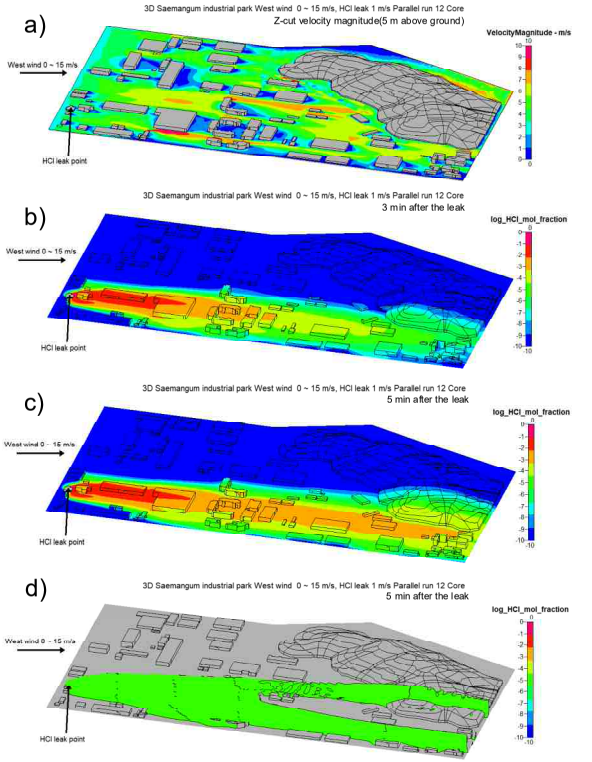

Figure4. Saemangum industrial park a) Velocity magnitude, b) 3 min after the HCl leak accident, c) 5 min after the HCl leak accident, d) HCl spatial distribution

5. Conclusion

- 5 minute after the accident, the HCl concentration appears at about 320 ppm in an area of 1,800 m width and 400 m length. This concentration is immediately harmful to the human body.
- Log HCl mol fraction: 10-6 → about 2.53 ppm, Therefore to evacuate to the permit exposure limit concentration (5 ppm) area, it is necessary to evacuate about 2 ~ 3 km away from the accident site.

6. Reference

- JaeYeol Lee, DongHyun Kim, SoonHee Ban, ChangJun Lee(2018), A Study of the Distance between a Tank and a Dike Considering a Leakage Velocity at an Opening Hole in case of a Leakage Accident, J. Korean Saf., Vol. 33, No. 5, 2018
- Choi, Goo (2009), Application CFD in the Atmospheric Dispersion(II) – The Effect of Complex Terrain on the Pollutant Dispersion, KOSAE, 2009.5, 512-513

This work was supported by the National Research Foundation of Korea (NRF) grant funded by the Korea government(MSIT)(No. 2019H1D8A1109814)

Disaster Prevention Awareness Questionnaire Survey for Residents of Storm Surge Hazard Area - A Case Study of Ube City, Yamaguchi Prefecture –

A. TAMURO, R.KUWAHARA and H.MURAKAMI

Yamaguchi University, Japan

1.Background and purpose

Natural disasters occur in various places in Japan every year. Large-scale flooding occurred due to heavy rains in western Japan in 2018, and it is essential for individuals to take disaster countermeasures. In this study, we conduct a questionnaire survey for residents of storm surge hazard area in Ube City, Yamaguchi Prefecture. As a result, we will clarify individuals' awareness of disaster prevention and elucidate the factors that affect disaster prevention awareness.

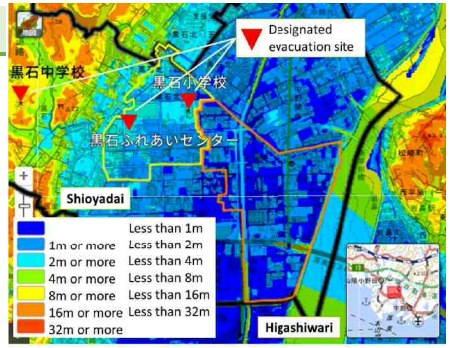

2.Survey Overview

Survey location
Kuroishi District, Ube City, Yamaguchi Prefecture (Higashiwari and Shioyadai Neighborhood Association)

Number of distributions 665

Responses 357 (response rate 54%)

Period October 30 to December 3, 2020

How to respond Questionnaire form, Internet

Number of questions 29 questions

Questions
I. Housing
II. Everyday Preparation
III. Response to Typhoon 2010

3.Survey results (comparison by neighborhood association)

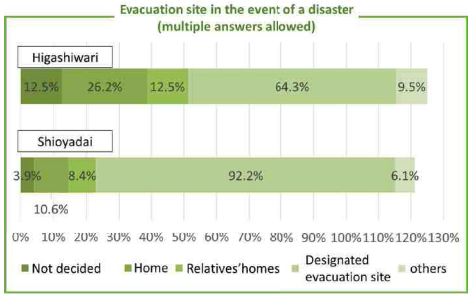

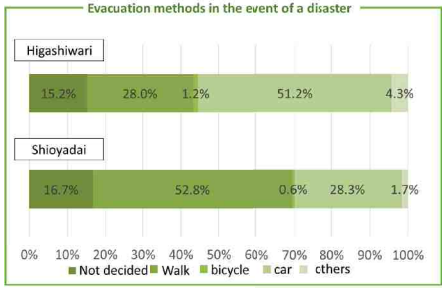

✓As for evacuation sites in the event of a disaster, there are more home evacuations than in the Shioyadai area. On the other hand, in the Higashiwari area, where rivers are close and designated evacuation sites are far away.

✓In the Shioyadai area, where designated evacuation sites are close, most say they will evacuate to designated evacuation sites.

✓As for the means of transportation, there are many walking at Shioyadai where shelters are relatively close, and there are many people who travel by car in Higashiwari, where evacuation shelters are far away. It can be seen that the means of transportation are different depending on the distance to the shelter.

4.September 2020 Typhoon No. 10 Haishen

From September 5th to 7th, a large and very strong force approached Kyushu. A very strong wind was observed mainly in Kyushu, and it became a record storm exceeding the value of the first place in the observation history. Heavy rains were caused on the Pacific side of western and eastern Japan, away from the center of the typhoon. The storm and heavy rains caused human damage, damage to homes, power outages and water outages.

In Ube City

9/6	13:00	Opening of evacuation center
	15:00	Start of evacuation preparations and evacuation for the elderly
		Up to 633 evacuees *Including voluntary evacuation
9/7	2:00	Power outages up to 19,150 homes
	10:10	Cancellation of issue

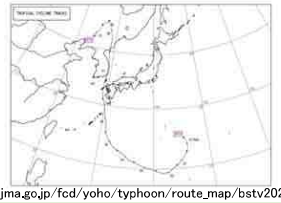

http://www.data.jma.go.jp/fcd/yoho/typhoon/route_map/bstv2020.html

5.Survey results (comparison by age)

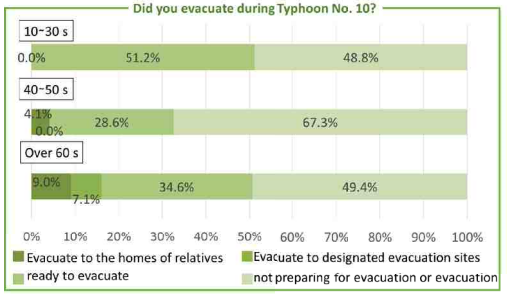

✓When choosing to live, 58.1% of people in their 10s and 30s said they had examined hazard maps and past disasters, compared with about 20% in other age years. It can be said that the younger generation is more aware of disaster prevention. Half of those in their 10s and 30s were evacuated but prepared to evacuate, and 13% in their 60s and above. In the Kuroishi area, evacuation preparations have not been issued, and this value is high even though it is a voluntary evacuation.

6.Conclusion

➢From the results of evacuation sites and evacuation methods in the event of a disaster, it was found that there were differences in the distance to rivers and evacuation sites, the selection of emergency evacuation sites, and the means of transportation in the event of emergency evacuation.

➢It was found that the younger generation had a higher rate of confirmation of hazard maps and a higher awareness of disaster prevention, such as preparing for evacuation before a disaster occurred. This may be due to the fact that hazard maps have become increasingly important in recent years and that publishing has accelerated. In addition, it is thought that many elderly people who live in this area from time to time do not examine the hazard map.

➢The high rate of confirmation of hazard maps and the actions taken during Typhoon No. 10 Haishen in 2020 showed that not only the elderly but also young people were more aware of disasters.

A Graph Theory-based User Association Scheme for Device-to-Device Task Offloading in 5G Networks

R.V. Dayot and I. Ra

(Kunsan National University, South Korea)

1 BACKGROUND

- ✓ Faster Data Transmission
- ✓ Improved Connectivity
- ✓ Higher Bandwidth
- ✓ Lower Latency

5G Features

URLCC | mMTC | eMBB

The Fifth Generation (5G) of mobile networks has brought upon a wide array of services that have revolutionized our experience with mobile computing and the Internet-of-Things (IoT).
By providing enhanced connectivity, ultra-low latency, and faster data transmission rates, services such as Virtual Reality (VR), Augmented Reality (AR), Vehicle-to-Everything Communication (V2X), IoT, and Smart Cities have been either enabled or improved.

5G Applications

Disaster Response | e-Health | Augmented Reality (AR) | V2X Comms

Artificial Intelligence | Smart Cities | IoT | Virtual Reality (VR)

2 PROBLEM

- ▲ Increased Data Traffic
- ▲ Energy Efficiency
- ▲ Effective Resource Allocation

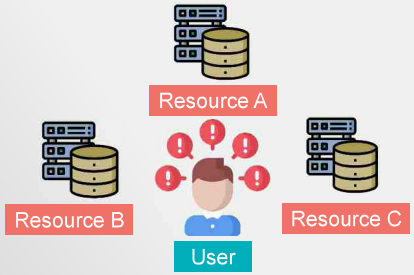

The challenge is how to **efficiently assign resources** to users in order to address the aforementioned problems.

3 OUR CONTRIBUTION

A **graph theory-based user association scheme** for assigning user tasks to network reso1urces. We find the "**best estimate**" routes from a user to a resource by considering the **availability of a resource**, **distance**, and **task size** to address the identified problems.

4 PROPOSED TASK OFFLOADING SCHEME

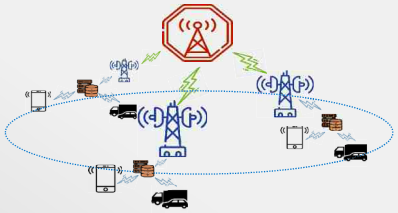

(Proposed 5G Network Model in this study)

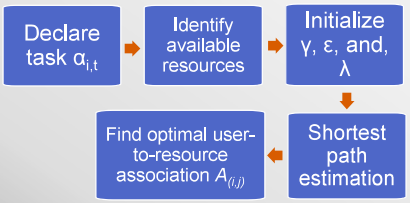

(User Association and Resource Allocation Process Flow)

- ❑ The 5G network is model as a graph $G = (V, E)$ that consists of a set of vertices and edges, V and E, respectively.
- ❑ When finding the shortest path from i to j (or l), we adapt the Bellman-Ford algorithm which calculates consecutive refinements of the vertex distances and processes them in every iteration.
- ❑ The best estimate route is calculated as $\boldsymbol{\beta(j) = min\{\beta(i) + w_{ij}\}, j \neq 0}$.
- ❑ By estimating the shortest path from a user to an available resource we can identify the optimal user association that can reduce energy consumption and transmission delay.

5 CONCLUSION

- ❑ A user to resource association scheme based on graph theory which is intended for efficient task offloading in a 5G network is presented in this work.
- ❑ In the future, application of the proposed scheme to different 5G use-case scenarios will be performed.

6 REFERENCES

[1] J. Navarro-Ortiz, P. Romero-Diaz, S. Sendra, P. Ameigeiras, J. J. Ramos-Munoz, and J. M. Lopez-Soler, "A Survey on 5G Usage Scenarios and Traffic Models," IEEE Communication Survey Tutorials, vol. 22, no. 2, pp. 905–929, 2020.
[2] S. O. Oladejo and O. E. Falowo, "Latency-Aware Dynamic Resource Allocation Scheme for Multi-Tier 5G Network: A Network Slicing-Multitenancy Scenario," IEEE Access, vol. 8, pp. 74834–74852, 2020.
[3] H. Halabian, "Distributed Resource Allocation Optimization in 5G Virtualized Networks," IEEE J. Selected Areas in Communications, vol. 37, no. 3, pp. 627–642, 2019.
[4] L. Tang, Q. Tan, Y. Shi, C. Wang, and Q. Chen, "Adaptive Virtual Resource Allocation in 5G Network Slicing Using Constrained Markov Decision Process," IEEE Access, vol. 6, pp. 61184–61195, 2018.
[5] Q. Yao, H. Yang, B. Yan, B. Bao, A. Yu, and J. Zhang, "Routing and Resource Allocation Leveraging Self-Organizing Feature Maps in Multi-core Optical Networks Against 5G and beyond," 2020 International Wireless Communications and Mobile Computing IWCMC 2020, pp. 857–860, 2020.
[6] M. Lin, Q. Ye, and Y. Ye, "Graph theory-based mobile network insight analysis framework," 2016 IEEE 7th Annual Ubiquitous Computing, Electronics, and Mobile Communications Conference UEMCON 2016, October 2016, 2016

2021
Proceedings of the
13th Joint Seminar